# Critical Role of $Ca^{2+}$ Current Facilitation in the Short-Term Facilitation of Purkinje Cell – Purkinje Cell Synapses

DOCTORAL DISSERTATION

A thesis submitted in partial fulfillment

of the requirements for the degree of

Doctor of Philosophy

By:

Françoise Díaz-Rojas

Supervisor:

Dr. Takeshi Sakaba

Co-Supervisor:

Dr. Shin-ya Kawaguchi

Graduated School of Brain Science

Doshisha University

March 2016

Kyoto, Japan

# Abstract

Short-term facilitation (STF) of synaptic transmission plays a critical role in neural information processing. Several hypotheses have been proposed to explain this process: temporal summation of residual $Ca^{2+}$, modulation of action potential (AP) waveform, saturation of $Ca^{2+}$ buffer proteins, facilitation of $Ca^{2+}$ current ($I_{Ca}^{2+}$) through voltage-gated $Ca^{2+}$ channels, and $Ca^{2+}$-dependent positive modulation of vesicle release machinery. We attempted to clarify the mechanism mediating STF at GABAergic synapses between cerebellar Purkinje cells (PCs) using dissociated rat cerebellar cultures. We performed fluorescent imaging of residual $Ca^{2+}$ increase upon an action potential in PC axon terminals using OGB-1 or OGB-6. PC terminals exhibited only a tiny increase in the fluorescence intensity upon stimulation single AP. With this information, we estimated the residual $Ca^{2+}$concentration, which could explain only 1% of the facilitation. Alternatively, direct patch-clamp recording from a PC axon terminal showed that presynaptic $I_{Ca}^{2+}$ was facilitated depending on the intracellular $Ca^{2+}$concentration upon paired pulses of AP-like waveforms. Application of BAPTA but not EGTA suppressed the facilitation of $I_{Ca}^{2+}$ suggesting that this facilitation is tightly coupled with $Ca^{2+}$ influx. Taking it into consideration that synaptic transmission shows about $4^{th}$ power dependency on the presynaptic $Ca^{2+}$ concentration, the $I_{Ca}^{2+}$ facilitation almost completely explained the facilitation of IPSCs at PC-PC synapses. Importantly, suppression of the $I_{Ca}^{2+}$ facilitation by modulation of the AP waveforms eliminated the facilitation of IPSCs. Our data suggests that the $Ca^{2+}$-dependent facilitation of the presynaptic $I_{Ca}^{2+}$ fully accounts for the synaptic facilitation observed at the PC-PC synapse.

# Acknowledgments

First, I would like to express my sincere gratitude my advisors, Dr. Shin-ya Kawaguchi and Dr. Takeshi Sakaba for their support, invaluable guidance and teachings, and all the aid I received from then during the development of this research and the writing of this document.

I would also like to thank to Dr. Mitsuharu Midorikawa and Dr. Tomoyuki Takahashi for their helpful comments and proofreading of the published manuscript of the results of this research. I also extend my feelings of gratitude to my thesis reviewing committee: Dr. Shigeo Takamori, Dr. Nobuyuki Nukina, and Dr. Yasuhiko Saito, for their insightful comments and encouragement, but also for the hard questions, which incented me to widen my research from various perspectives.

My deepest gratitude to MEXT, the Government of Japan and Doshisha University for their financial and logistical support in the realization of my studies and research here in Doshisha University.

Finally, I would like to thank my parents and my friends for the unceasing encouragement, support and attention. I am also grateful to my partner who supported me through this venture.

# Table of Contents

# Table of Figures

# Abbreviation list

AP: Action potential.

$Ca_{free}$: Free (unbound) $Ca^{2+}$ ions in the cytosol of the presynaptic terminal.

CaM: Calmodulin.

CNS: Central nervous system.

DCN: Deep cerebellar nuclei.

EGFP: Enhanced green fluorescence protein.

GC: Granule cell.

$I_{Ca}{}^{2+}$: $Ca^{2+}$ current.

IN: Interneuron.

NT: Neurotransmitter.

OGB: Oregon Green BAPTA.

PC: Purkinje cell.

PPD: Paired-pulse depression.

PPF: Paired-pulse facilitation.

PPR: Paired-pulse ratio.

PSC: Postsynaptic currents.

PSP: Postsynaptic potentials.

STF: Short-term facilitation.

VDCC: Voltage-dependent $Ca^{2+}$ channels.

# Chapter 1. Introduction

## 1.1. Basis of Synaptic Transmission

When the presynaptic terminal of a chemical synapse is activated by the arrival of an action potential from the neuronal axon, its voltage-dependent $Ca^{2+}$ channels open, allowing the influx of $Ca^{2+}$ into the terminal. Some of these $Ca^{2+}$ ions can be quickly bound by a series of calcium-binding proteins that help regulating the effective concentration of $Ca^{2+}$ ions in the cytoplasm of the synaptic terminal. The unbound $Ca^{2+}$ ions ($Ca_{free}$) initiate then the vesicle release process by binding to synaptotagmin, a $Ca^{2+}$ sensor protein found on the membranes of the synaptic vesicles (Südhof, 2013). The synaptic vesicles, already docked at the membrane and ready for release, can then start fusing with it, which results in the release of the neurotransmitter (NT) into the synaptic cleft. From there, the NT reaches the postsynaptic cell and binds to specialized receptors on the cell membrane, which induces the opening of ion channels or activates messenger pathways that ultimately excite or inhibit the cell (see Fig. 1).

A small fraction (from a hundredth to a thousandth) of the $Ca^{2+}$ ions that entered the presynaptic terminal remains unbound (Neher and Augustine 1992; Tank *et al.* 1995). This unbound $Ca^{2+}$, or residual $Ca^{2+}$ ($Ca_{res}$), is then slowly (hundreds of milliseconds to seconds) removed from the presynaptic terminal. In addition, the buffered $Ca^{2+}$ is also slowly unbound from the $Ca^{2+}$ buffers, adding to the residual $Ca^{2+}$.

### 1.2.1. Synaptic vesicles and release machinery

Not all synaptic vesicles are ready to be released upon the arrival of an AP to the terminal. In general, vesicles can be grouped into distinct groups, or more often pools, based on their function and location inside the presynaptic terminal. The readily releasable pool (RRP) is generally composed by those vesicles docked in the active zone. These vesicles will be the first one to be released upon AP arrival, and a fraction of released vesicles in response to an AP, usually termed release probability, (Pr) depends on the synapse. This pool is often small and quickly exhausted during repetitive stimulation (Richards *et al.*, 2003, Rizolli and Betz, 2005, Delgado *et al.*, 2000). A second pool is the recycling pool (RcP), composed by vesicles that are close to the cell

membrane, but are not necessarily docked. Physiological stimulation will maintain constant release, with the pool being continually refilled by newly recycled vesicles (Richards *et al.*, 2003, Rizolli and Betz, 2005). Finally, the reserve pool (ReP) is mainly all the other vesicles in the terminal (typically 80 ~ 90% of all vesicles in the terminal). These vesicles may never be recruited during physiological stimulation, and only external, sustained stimulation can induce release of the vesicles in this pool (Fig 1).

Thus, when an AP invades the presynaptic terminal, voltage-dependent $Ca^{2+}$ channels will open allowing the flux of $Ca^{2+}$ into the terminal. As described above, the free $Ca^{2+}$ will then bind to synaptotagmin and initiate the vesicle fusion process. In this step, SNARE proteins fuse the membranes of the synaptic vesicles with the presynaptic cell membrane to allow the exocytosis of the NT into the synaptic cleft. Following the release of NT, the synaptic vesicle is quickly recycled for future reuse.

Transmitter released from the presynaptic terminal acts on the postsynaptic receptors and causes postsynaptic responses. Depending on the receptor types, the responses are either excitatory or inhibitory.

### 1.2.2. Role of $Ca^{2+}$

From the entire process of synaptic transmission, it is important to highlight two points. The first point is the relation between the $Ca_{free}$ and the amount of NT released. Because $Ca^{2+}$ binds to multiple low-affinity binding sites of synaptotagmin (Jahn *et al.* 2003; Schneggenburger and Neher 2005; Sudhof and Rothman 2009), there is a steep dependency between the $Ca_{free}$ and the NT released. This supra-linear relation has been reported to be approximately a fourth-power relation (Katz and Miledi, 1968, Zucker *et al.* 1986, Augustine and Charlton, 1986, Kits and Mansvelder, 2000).

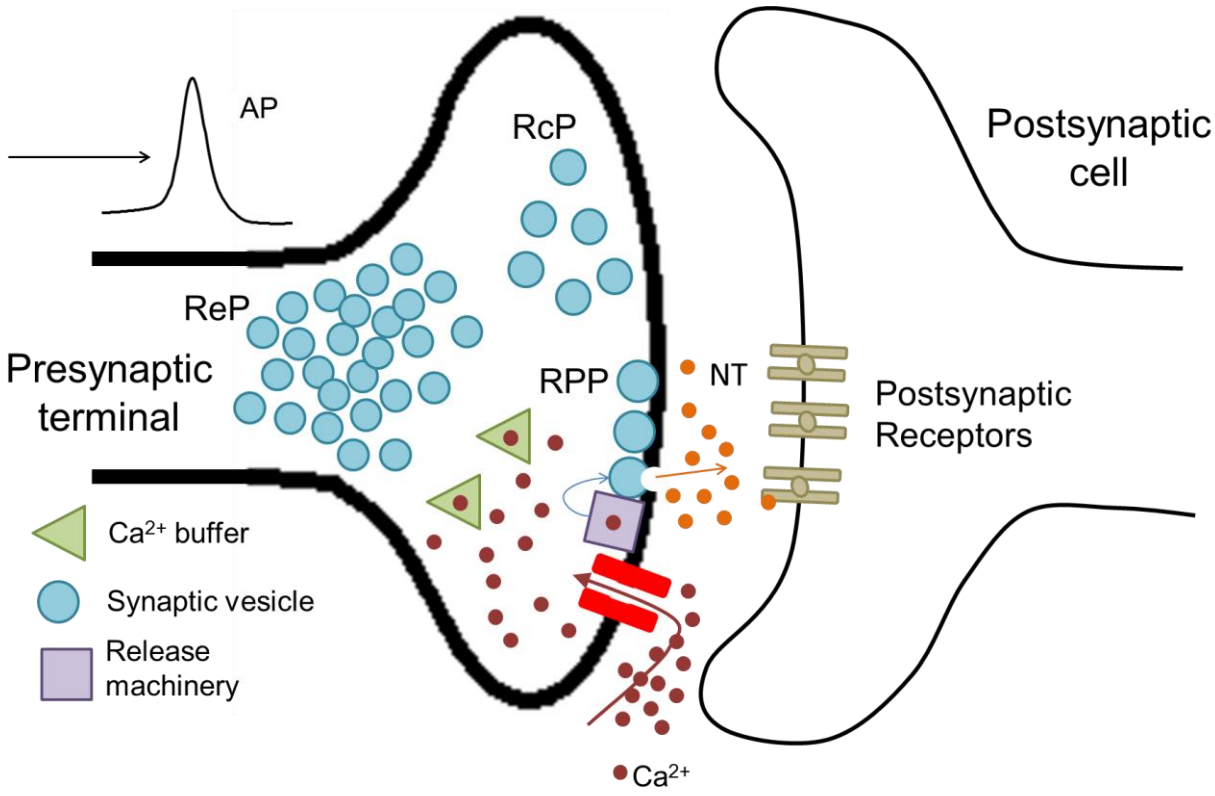


**Figure 1. Synaptic release process.** The arrival of an action potential (AP) to the presynaptic terminal causes the opening of voltage-dependent Ca2+ channels (in red) that start the synaptic vesicle release processes, which ultimately ends with the release of neurotransmitter (NT) and the stimulation of the postsynaptic cell through specialized receptors in the postsynaptic cell membrane. RPP: Readily releasable vesicle pool. RcP: Recycling vesicle pool. ReP: Reserve vesicle pool.

The second point is the stochastic nature of NT release. NT is released in a probabilistic manner in small, discrete packages or "quanta" (amount of NT in a single vesicle release), reflected by the release probability of each synaptic vesicle (Fatt and Katz, 1952, Branco and Staras, 2009). Due to this stochastic nature, NT is sometimes spontaneously released even in the absence of AP with very low probability (Lin *et al.*, 1990, Littleton *et al.*, 1994, Kaeser and Regehr, 2014). These spontaneous events cause a phenomenon originally termed miniature end-plate potentials (Fatt and Katz, 1952), or the smallest amount of stimulation that one neuron can send to another neuron. Referred more generally as miniature postsynaptic potentials (PSP) (miniature postsynaptic currents (PSC) in the case of voltage-clamp recordings), they provide an important measurement of the release properties of the presynaptic terminal (Sakaba and Neher, 2001, Scheuss and Neher, 2001, Yang and Xu-Friedman, 2013).

Synaptic transmission can be classified either as excitatory or inhibitory, depending on whether the NT causes the postsynaptic cell membrane to depolarize or to hyperpolarize, respectively. At the CNS, excitation is commonly mediated by glutamate (Meldrum, 2000) binding to receptors in the postsynaptic cell's membrane that cause the opening of cation channels (Dingledine *et al.*, 1999, Cull-Candy *et al.*, 2001). Inhibition is usually mediated by γ-Aminobutyric acid (GABA) and glycine, causing the opening of $Cl^-$ channels upon binding to postsynaptic receptors (Macdonald and Olsen, 1994, Hevers and Lüddens, 1998).

## 1.2. Short-term Synaptic Plasticity

Repeated activation of a synapse may lead to a phenomenon called short-term synaptic plasticity, in which the synaptic transmission is transitorily strengthened or weakened by the recent activity of that synapse (Zucker and Regehr, 2002; Abbott and Regehr, 2004; see Fig. 2). Short-term synaptic plasticity arising due to presynaptic mechanisms (increase or decrease of NT released) has been termed short-term presynaptic plasticity (Fioravante and Regehr, 2011; Regehr, 2012). Conversely, short-term postsynaptic plasticity refers to the synaptic plasticity observed due to postsynaptic mechanisms. For example, saturation and desensitization of the postsynaptic receptors may transitorily weaken the synaptic transmission (Regehr, 2012).

### 1.2.1. Short-term Presynaptic Plasticity

As it was briefly explained above, repeated stimulation of the presynaptic terminal may lead to a phenomenon called short-term presynaptic plasticity, in which the amount of NT released by the presynaptic cell is transitorily modulated by the recent activity of that synapse (Zucker and Regehr, 2002; Abbott and Regehr, 2004; Fioravante and Regehr, 2011; Regehr, 2012). The duration of this modification varies from cell to cell and is dependent on the type of stimulation, but it's typically in the range of tens of milliseconds to minutes.

Depending on whether the amount of neurotransmitter is increased or decreased, we can classify the presynaptic short-term plasticity into two broad categories: short-term

synaptic enhancement and short-term depression (Regehr, 2012).

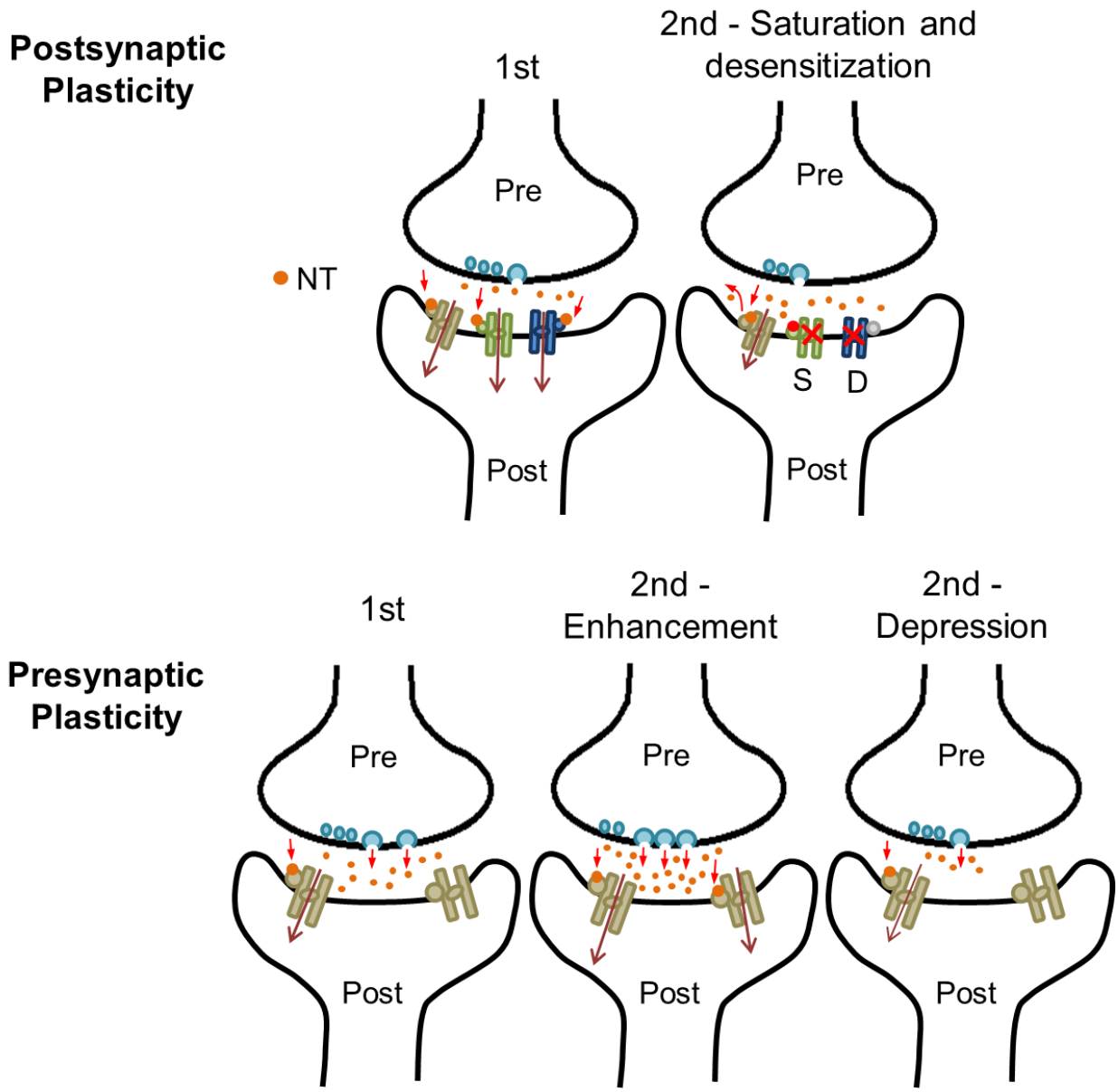


**Figure 2. Short-term synaptic plasticity.** Modifications of the synaptic transmission in the short-term can be presynaptic or postsynaptic in origin. Top: Postsynaptic mechanisms. Short-term postsynaptic plasticity may occur as a result of saturation (S) or desensitization (D) of postsynaptic receptors. Bottom: Presynaptic plasticity. Enhancement is the increase of NT released, while depression is the decrease. Red arrows: movement of NT. Purple arrows: influx of ions through ionic channels. Orange dots: NT. Blue circles: synaptic vesicles.

Short-term enhancement can in turn be categorized in three groups: facilitation, augmentation and post-tetanic potentiation. In all three cases, the NT released from the presynaptic terminal after repeated stimulation is increased. The main difference lies in the time courses. Facilitation usually lasts in the range of tens of milliseconds

to hundreds of milliseconds; augmentation is in the order of seconds; post-tetanic potentiation is in the order of tens of seconds to minutes (Regehr, 2012). It is also important to note that both augmentation and post-tetanic potentiation are caused by sustained activation at high frequency of the presynaptic terminal (Regehr, 2012).

For the scope of this research, we will be focusing on depression and facilitation.

### 1.2.2. Paired-Pulse Facilitation and Depression

As a form of short-term facilitation, activation of the presynaptic terminal by two closely spaced action potentials, usually within a second, can lead to an increase in NT released, a phenomenon called Paired-Pulse Facilitation (PPF, Fig. 3, top; Katz and Miledi, 1968; Thomson, 2000, Regehr, 2012). An opposite phenomenon, in which the amount of NT released is instead decreased after a paired stimulation, may also occur. This is called Pair-Pulse Depression (PPD, Fig. 3, bottom; O'Donovan and Rinzel, 1997), a form of short-term depression.

The degree of PPF and PPD can be measured by the ratio of the second PSC over the first, a value that is termed paired-pulse ratio (PPR). For both PPF and PPD, the PPR is dependent on the interval between the stimulation pulses (Fig 2. Right) and the longer the interval, the weaker the effect (PPR approaches 1).

Both PPF and PPD play an important role in neural signaling processing (Zucker, 1989, Stopfer and Carew, 1996, Fisher, *et al.*, 1997, Varela *et al.* 1999, Buonomano, 2000, Dittman, *et al.*, 2000, Fortune and Rose, 2001). One physiological role in neural signaling processing is band-pass filtering. Facilitation works as a high-pass filter, as only the presynaptic inputs that arrive at the presynaptic terminal closely matched in time (i.e. occur at a high frequency) will produce a heightened response in the postsynaptic cell. Conversely, those presynaptic inputs in the terminal that are spaced one from the other will only produce the basal response on the postsynaptic cell. This filter can help the cell discern between incoming patterns of activity. In a likewise yet opposite role, depression works as a low-pass filter, attenuating those inputs that arrive at the presynaptic terminal closely matched in time, while allowing those sparsely matched to be transmitted in full to the postsynaptic cell (Fortune and Rose, 2001, Silver, 2010).

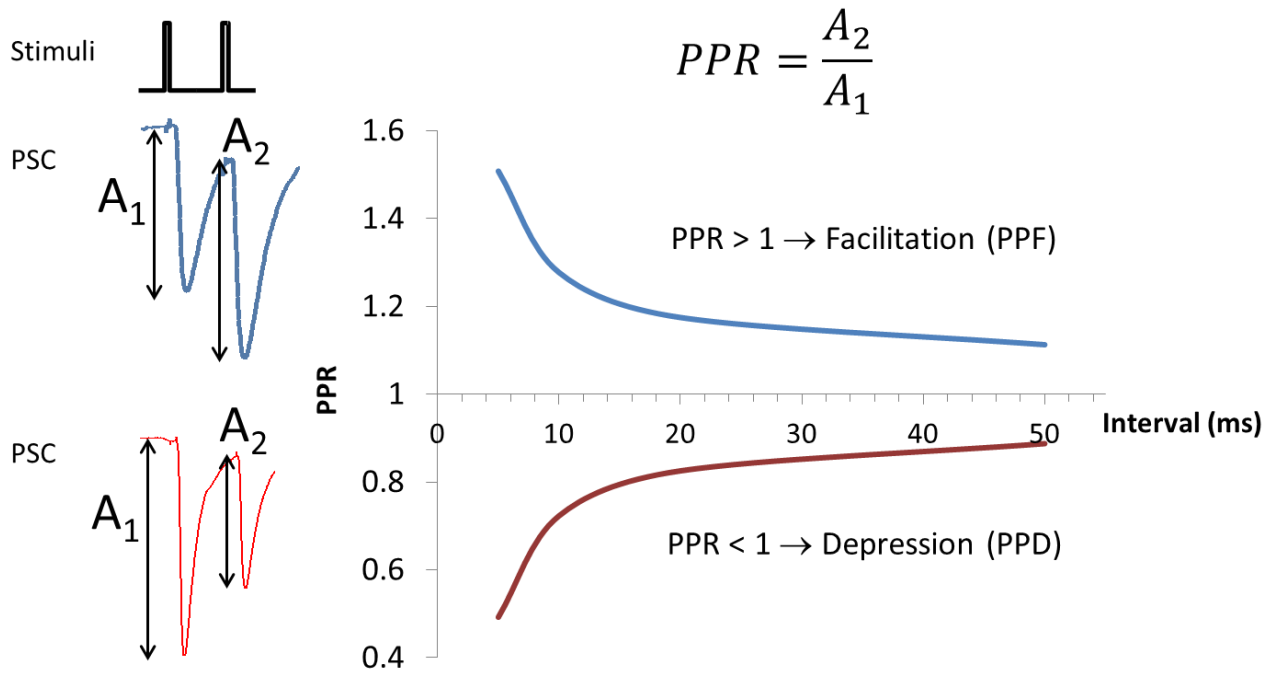


**Figure 3. Paired-pulse facilitation/depression.** One form of short-term plasticity (STP) is paired-pulse facilitation/depression, in which the response of the postsynaptic cell to a second stimulus delivered shortly after a first gets facilitated/depressed. Facilitation or depression can be reflected by the ratio of the amplitude of the second PSC over the first, called paired-pulse ratio (PPR). In general, PPF and PPD are dependent on the frequency of stimulation, with higher frequencies causing a stronger effect.

In the same way, facilitation and depression may help with input integration from multiple sources. Inputs paired in time will produce a stronger response (for example, stronger excitation, or reduced inhibition) in the postsynaptic cell (Volman *et al.*, 2009, Izhikevich *et al.,* 2003).

Another role of short-term plasticity is the coding/decoding of temporal information, by means of the frequency between inputs in the presynaptic cell, which in turn translates to a wide range of responses (PSC) in the postsynaptic cell (Buonomano, 2000).

In the auditory pathways, another role of short-term plasticity has been reported. Opposite types of plasticity in a single neural circuit allows the discrimination between lateral inputs (right/left) used in sound-source localization (Abott and Regehr, 2004).

*Mechanisms Underlying Short-Term Plasticity*

PPD has mainly been attributed to a high initial probability of NT release (Liley and North, 1953; Betz, 1970; Zucker and Regehr, 2002, Regehr, 2012). In short, the high release probability produces depletion of readily releasable pool of synaptic vesicles, which cause less and less NT to be released at each activation. Other mechanisms have also been observed, such as low excitability of the presynaptic cell membrane (Kawaguchi and Sakaba, 2015), inactivation of $Ca^{2+}$ channels (Xu and Wu, 2005), and inactivation of release sites (Betz 1970; Varela *et al.* 1997; Neher and Sakaba 2008).

Despite the extensive research done in this field, the mechanism underlying PPF still remains unclear, particularly at inhibitory GABAergic synapses. The classical hypothesis for an underlying mechanism, proposed by Katz and Miledi (1968), involves the temporal summation of $Ca^{2+}$ transients into the terminal upon repeated activation (Fig 2A). Due to the relatively slow dynamics of $Ca^{2+}$ inside the terminal, the residual concentration of $Ca_{free}$ may be momentarily higher as subsequent action potentials arrive. If we assume the $Ca^{2+}$ influx into the terminal is the same at each depolarization, then the total $Ca_{free}$ will be subsequently higher during the second stimulation, producing an increase in the release of neurotransmitter.

Because it has been shown that $Ca_{free}$ is strongly related with the neurotransmitter released in a fourth power manner, even a small increase in the total $Ca_{free}$ due to accumulation of residual $Ca^{2+}$ may result in a substantial increase of NT released if the initial vesicle release probability is sufficiently low.

A second hypothesis that has been proposed to explain this phenomenon is the saturation of endogenous $Ca^{2+}$ buffers (Fig. 4B). Some endogenous $Ca^{2+}$ chelator molecules, like calbindin, quickly capture the ions that flux into the terminal upon depolarization in order to regulate $Ca_{free}$ in the presynaptic terminal. If the amount of $Ca^{2+}$ ions that flow into the cell is large enough, temporary local buffer saturation around $Ca^{2+}$ channels may occur. Thus, when the second AP invades the terminal, the effective concentration of endogenous $Ca^{2+}$ buffers is lower than that at the first AP, which leads to a comparative increased $Ca_{free}$ around the transmitter release zone. This in turn leads to an increased NT release (Neher 1998; Rozov *et al.* 2001; Blatow *et al.* 2003; Felmy *et al.* 2003; Matveev *et al.* 2004).

On the other hand, there also exist slow endogenous $Ca^{2+}$ buffers, like parvalbumin, which accelerate the decay of the residual $Ca^{2+}$ in the presynaptic terminal (Muller *et al.* 2007). Saturation of this type of slow calcium-binding proteins may be more difficult, and due to the release/binding dynamics, its effects on short-term plasticity may be harder to discern. In two particular studies in parvalbumin knockout mice, which may provide a parallel to the saturation condition, short-term depression is transformed into facilitation (Caillard *et al.*, 2000; interneuron to PC synapse) or the decay of facilitation was slowed (Muller *et al.*, 2007; calyx of Held synapse).

A third possibility is that the facilitation of synaptic transmission is mediated by facilitation of the $Ca^{2+}$ influx into the presynaptic terminal upon depolarization (Fig. 4C). It has been previously reported that some voltage-dependent $Ca^{2+}$ channels can be facilitated in an activity-dependent manner. In the previous two hypotheses, it is assumed that the influx of $Ca^{2+}$ into the terminal remains constant upon repeated stimulation. This is not necessarily the case, however, as previous studies have shown. A particular study by Hori and Takahashi (2009) showed that in the calyx of Held synapse, when facilitation of $Ca^{2+}$ currents is suppressed, the facilitation of synaptic transmission diminishes in about 50%. Additionally, it has been shown that a certain types of $Ca^{2+}$ channels, P/Q-type voltage-dependent calcium channels (see section 1.2.2), which facilitate in a $Ca^{2+}$-dependent manner, play a role in short-term facilitation (Forsythe *et al.* 1998, Inchauspe *et al.*, 2004, Mochida *et al.*, 2007). A variant of this hypothesis is the broadening of AP waveforms in an activity-dependent manner, for example, due to inactivation of $K^+$ channels (Geiger and Jonas, 2000).

An unidentified $Ca^{2+}$ sensor for facilitation accounts for a fourth hypothesis (Fig. 4D). It is possible that there may be a different $Ca^{2+}$ sensor than synaptotagmin-1/2 (Stanley 1984; Bain and Quastel 1992; Yamada and Zucker 1992; Atluri and Regehr 1996; Bertram *et al.* 1996). Synaptotagmin-1/2, a sensor for evoked transmission, is relatively insensitive to residual calcium, due to its fast, low-affinity $Ca^{2+}$ binding dynamics. However, it is possible that there exists a different type of $Ca^{2+}$ sensor with opposite dynamics to synaptotagmin-1/2 that may cause facilitation.

A fifth possibility may be rapid recruitment of releasable vesicles to the active zone (Fig. 4E). Activity-dependent increase in release sites or rapid recruitment of reluctant releasable vesicles may augment the effective number of releasable vesicles at the

active zone upon repeated stimulation (Valera *et al.*, 2012, Brachtendorf *et al.*, 2015), producing an increase in NT released, and thus facilitated synaptic transmission.

It is important to note that a single synapse is not limited to a single mechanism mediating plasticity; instead, most synapses have interplay between various mechanisms of facilitation and depression, and the net result will depend on the properties of each synapse as well as stimulus patterns (Regehr, 2012).

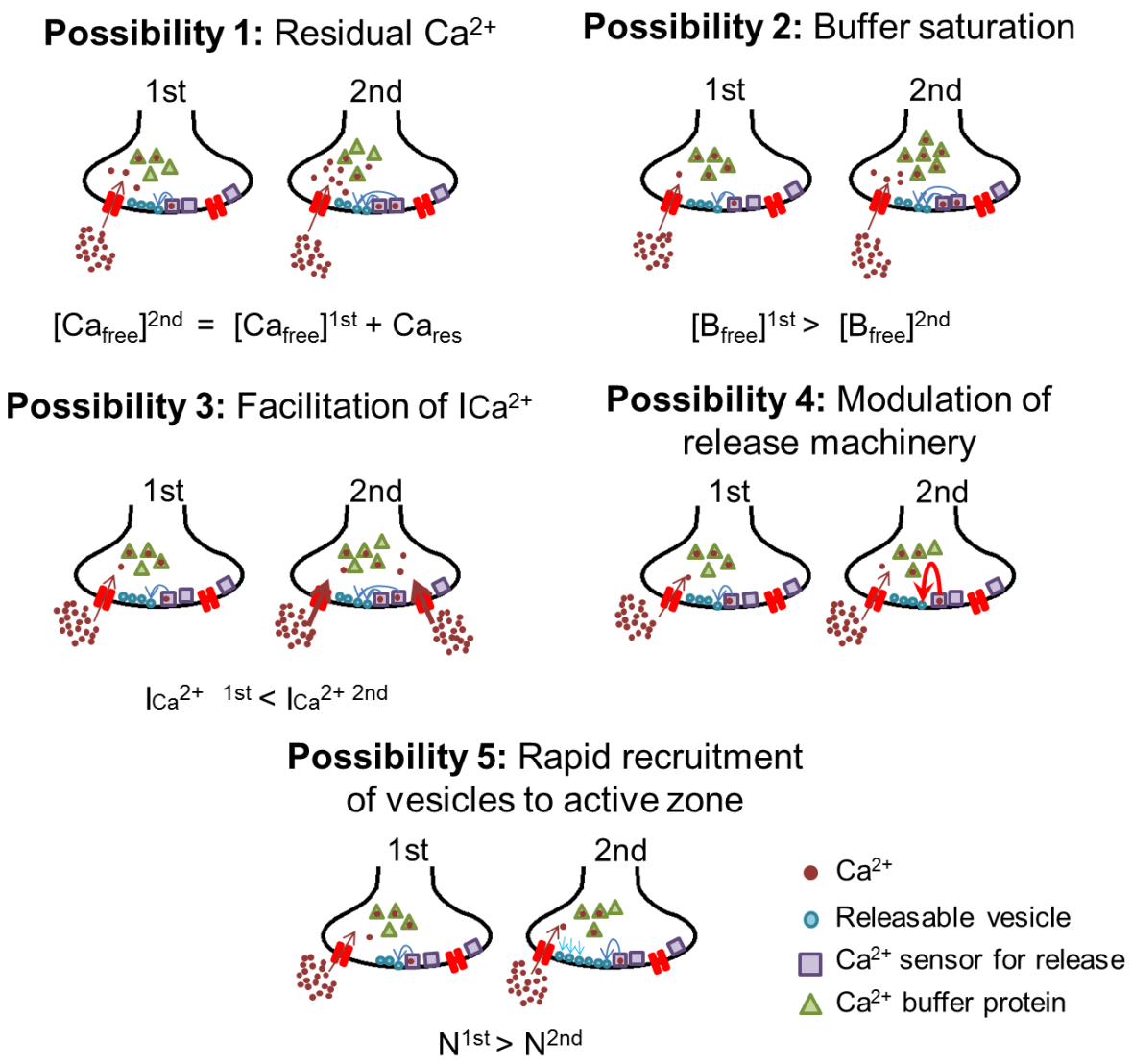


**Figure 4. Mechanisms proposed to explain STF.** Several hypotheses for a mechanism underlying STF have been proposed: temporal summation of residual $Ca^{2+}$ (possibility 1), saturation of endogenous $Ca^{2+}$ buffer proteins (possibility 2), facilitated $Ca^{2+}$ influx through voltage-gated $Ca^{2+}$ channels (possibility 3), $Ca^{2+}$-dependent positive modulation of vesicle release machinery (possibility 4), and rapid recruitment of vesicles to the active zone (possibility 5).

The study of short-term facilitation has been hindered by the small size of presynaptic terminals (Inchauspe *et al.*, 2004, Mochida *et al.*, 2007, Hori and Takahashi, 2009). For a correct and accurate assessment of the mechanisms underlying the short-term facilitation phenomenon at presynaptic terminals, direct access to the terminal is required. Patch-clamping of synaptic terminals in brain slices represents a difficult task for most synapses. Recordings from the cell's soma may not be able to dissect the effects taking place at synaptic terminal level, and current imaging techniques may not provide the required spatiotemporal resolution to analyze the biophysical properties involved in the NT release processes.

Therefore, to address the issue of the small size of presynaptic terminals, we studied short-term facilitation at cerebellar Purkinje cells (PC) in culture preparations. PCs extend axon collaterals to neighbouring PCs in the cerebellum. This connection shows short-term facilitation (Orduz and Llano, 2007, Bornschein *et al.*, 2013). Additionally, in our culture preparations, access to the synaptic terminals is relatively easier than in cerebellar slice, owing to the increased visibility to reduced surrounding tissue and the easiness of virus transfection, which allows fluorescence labeling of PCs.

## 1.3. Purkinje Cells and the Cerebellum Circuit

The cerebellar cortex is one of the best-characterized circuits of the central nervous system and is known to play a key role in the precise timing of motor control (Ivry, 2007, Watt *et al.*, 2009), integrating and processing motor and sensory information from many cortical and non-cortical sources (see Fig. 5A for a schematic of the cerebellar cortex circuit). The cerebellum receives its main input from the mossy fibers, which carry the sensory commands from the cerebral cortex and both cortical and non-cortical sensory information. Mossy fibers make synapses with the granule cells (GC), the most abundant cell in the CNS. GCs relay this information through their long axons, called parallel fibers, to the Purkinje cells (PC). These excitatory synaptic inputs are weak in amplitude but large in numbers. Up to 80 000 parallel fibers make synaptic contact on single PCs (Konnerth *et al.* 1990).

Through a different pathway, PCs receive a secondary excitatory input through the

climbing fibers, coming from the inferior olivary nucleus in the medulla oblongata. These inputs are strong, and generate a complex spike excitatory postsynaptic potential (EPSP) in PCs upon activation. However, each PC receives inputs from a single climbing fiber. These inputs are thought to represent the feedback motor command, either as an "error signal" or as a "teacher signal" (Ohtsuki *et al.*, 2009, Simpson *et al.*, 1996). They also play an important role in timing of motor control and non-motor cognitive functions (Simpson *et al.*, 1996, Xu *et al.*, 2006, Liu *et al.*, 2008).

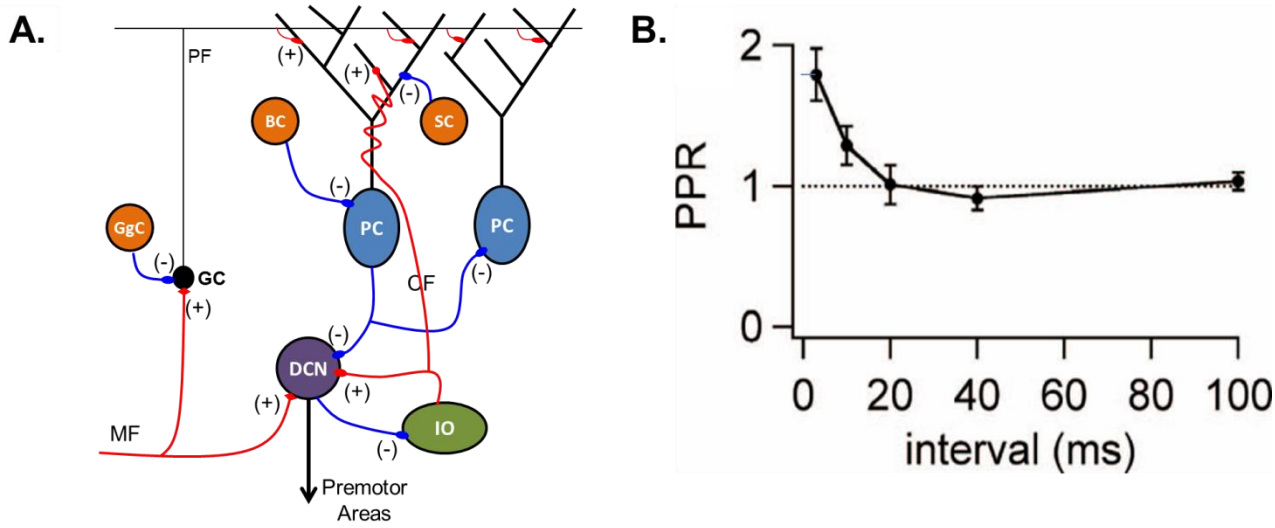


**Figure 5. Purkinje cell – Purkinje cell connection.** A. Schematic drawing of the cerebellar microcircuit. Sensory input through the mossy fibers (MF) arrive at granule cells (GC) in the cerebellar cortex. Granule cells, which also receive inhibitory inputs from Golgi cells (GgC), relay this inputs through the parallel fibers (PF) to the Purkinje cells. Parallel fiber input, together with the strong excitatory input from the climbing fibers coming from the inferior olive (IO) and the inhibitory inputs from the basket cells (BC) and stellate cells (SC), are integrated by the Purkinje cells to produce the single output of the cerebellar microcircuit to the deep cerebellar nuclei. PC axon collaterals targeting neighbouring PCs has been reported in slice in 10% of PC during early developmental stages. Excitatory synapses are shown as (+) and in red, inhibitory as (-) and in blue. B. Paired-pulse ratio at a PC – PC synapse. PC – PC synapse shows clear STF at frequencies from 300 – 20 Hz. Taken from Orduz and Llano, 2007.

PCs also receive inhibitory inputs from several inhibitory sources. The majority of these sources are inhibitory interneurons in the cerebellum (basket cells and stellate cells). In addition, inhibitory inputs from neighbouring PCs mainly present during

early developmental stage have also been reported (Gianola *et al.*, 2003, Orduz and Llano, 2007, Bornschein *et al.*, 2013; see below).

These synaptic circuits are the core of the cerebellum cortex. The core unit repeats across the entire cerebellar cortex in a highly organized manner, integrating and processing the motor and sensory inputs in order to output the modulations to the motor commands required for precise, target-oriented movements of the body.

These modulations are transmitted through the PCs. PCs are the sole output neurons of the cerebellar cortical circuit, and form inhibitory GABAergic synapses mainly on deep cerebellar nuclei (DCN) neurons, which in turn integrate the processed neural signal from the cerebellar cortex with those coming from other cerebral cortical areas to produce the main output of the motor commands from the brain to the lower motor nuclei in the spine cord.

In addition, it has been reported that PCs also target neighboring PCs through axon collaterals early in the developmental stage. Although this inhibitory synapse is initially depressing, it becomes facilitating at around 2-3 weeks after birth, before being almost eliminated altogether shortly after (Watt *et al.*, 2010, Orduz and Llano, 2007, Bornschein *et al.* 2013). In cerebellar slices, paired-pulse ratios for 3- and 20-ms stimulation intervals were 1.79 ± 0.18 and 1.01 ± 0.14, respectively. At longer intervals, the facilitation observed is below 5% (Fig 3B; Orduz and Llano 2007).

It is interesting to note that unlike PC synapses on another PC, PC – DCN neurons synapses exhibit potent short-term depression (Telgkamp and Raman 2002; Pedroarena and Schwarz, 2003). It remains elusive how the PC output synapses on a PC and those on a DCN neuron show opposite forms of short-term plasticity, i.e. facilitation and depression. Direct patch-clamp recording from PC axon terminals recently clarified that frequency-dependent attenuation of presynaptic APs underlies the depression of PC output synapses on DCN neurons (Kawaguchi and Sakaba 2015). Conversely, the mechanism underlying PPF at PC – PC synapses still remains unclear. Because PCs highly express two $Ca^{2+}$ buffering proteins, calbindin and parvalbumin, endogenous buffer saturation by increased $Ca_{free}$ during high-frequency stimulation may underlie PPF. However, recent research showed that genetic ablation of calbindin and/or parvalbumin in PCs have no significant effect on PPF (Bornschein *et al.* 2013). This leaves residual calcium, facilitation of $Ca^{2+}$ currents or $Ca^{2+}$-dependent

modification of release machinery as the possible mechanisms for PPF at this synapse. In this study, we attempted to discriminate the remaining possibilities that may underlie PPF at the PC – PC synapse.

## P/Q-type Voltage-dependent $Ca^{2+}$ Channels

The influx of $Ca^{2+}$ into the terminal is mediated by highly selective voltage-sensitive $Ca^{2+}$ channels, which preferentially allow the influx of $Ca^{2+}$ ions into the terminal upon membrane depolarization. These voltage-dependent $Ca^{2+}$ channels (VDCCs) are not only located in the synaptic terminal of CNS neurons, but in most of the excitable cells. VDCCs can be classified into different types depending on their biophysical properties and/or by the toxin they are inhibited. In this classification, we can find L-, N-, P/Q- R-, and T-type VDCCs. Each type is involved in a variety of specific physiological functions, ranging from vesicle release to muscle contraction, among others. Due to their involvement in vesicle release, it makes sense then to propose that the properties of these VDCCs may be related to the short-term plasticity processes present at many synapses.

P/Q-type VDCCs are a particular type of VDCC that play an important role in the vesicle release process in synaptic terminals in the CNS (Ishikawa *et al.*, 2005, Nimmrich and Gross, 2012). They were initially differentiated from other VDCC types by their susceptibility to be blocked by the toxin ω-agatoxin (ω-AGA). The P in their name comes from Purkinje cells, as they abundantly express P/Q-type VDCCs (Llinás *et al.*, 1989). Because P-type and Q-type are closely related, as they are produced from the same gene via alternative splicing, it is difficult to differentiate them. Thus, the channel has been labeled by both names, hence P/Q-type VDCC.

The structure of P/Q-type VDCC is composed of three subunits: the main pore-forming α1 subunit, an α2 subunit and a ß subunit. The α1 subunit is in turn composed of four domains, each containing six transmembrane (S1 ~ S6) spanning α helices. The S5 and S6 loops form the pore structure, whilst the S1 and S2 loops are thought to be responsible for the inactivation of the channel (Currie, 2010). Changes in the membrane potential are sensed by the S4 loop (Currie, 2010). The α2 and ß subunit regulate the kinetics and the expression level of the channel (Nimmrich and Gross,

2012). A calmodulin (CaM) association domain in the ß subunit has also been reported (Lee *et al.*, 1999). CaM is a small, highly conserved protein that contains two approximately symmetrical domains each containing a pair of EF-hand motifs (called the N- and C-domain) separated by a flexible linker region. Each EF-hand motifs can bind a $Ca^{2+}$ ion, which produces two distinct effects on $Ca^{2+}$ channels. $Ca^{2+}$ binding to the C-domain has been shown to increase the probability of the channel opening, while $Ca^{2+}$ binding to the N-domain produces a slow inactivation of the channel (Lee *et al.*, 2000).

The aim of this research is to elucidate the mechanisms mediating the facilitation property in the synapses between PC – PC by direct recording from the presynaptic terminal of PCs. In addition, simultaneous recordings from the presynaptic terminals and the postsynaptic cell would allow one to examine how each potential mechanism contributes to synaptic facilitation quantitatively. Because the study of STF in inhibitory neurons has been lacking, understanding the mechanisms underlying facilitation at this synapse may help understand STF in other synapses. Additionally, because PCs predominantly express P/Q-type VDCC channels, the findings of this research may also be applicable to other synapses in the CNS.

# Chapter 2. Materials and methods

***Culture preparations:*** Previous to the preparation of the cultured cells, we treated glass cover slips with HCl (2 M/l) for 72 hours. Following this, we thoroughly washed the cover slips and bathed them in poly-D-lysine for 24 hours prior to the culture preparation. On the day of the culture, the remaining poly-D-lysine was extracted, the cover slips were washed with double distilled water, and then submerged in Dulbecco's modified Eagle medium/Ham's F12-based medium, with 2.5% fetal bovine serum. The cover slips were set aside.

For the culture preparation, newborn rats were decapitated and their brains were removed. We dissected the cerebellums, removed the meninges and incubated them in $Ca^{2+}$ and $Mg^{2+}$-free Hanks' balanced salt solution with 0.1% trypsin and 0.1% DNase for 15 minutes at 37°C. Following the incubation period, the bathing solution was carefully replaced with $Ca^{2+}$-free Hanks' balanced salt solution with 0.1% DNase. Cells were then dissociated by trituration with a glass pipette and seeded on the poly-D-lysine-coated cover slips submerged in Dulbecco's modified Eagle medium/Ham's F12-based medium, with 2.5% fetal bovine serum. One day after the seeding, 75% of the medium was replaced with serum-free Eagle-based basal medium. One week after seeding, PCs were infected with adeno-associated virus (AAV) vector carrying enhanced green fluorescent protein (EGFP) under the control of CAG promoter (AAV-CAG-EGFP) (Kaneko *et al.*, 2011). The AAV vector was produced in HEK293 cells by transfection with AAV-CA-EGFP (Kaneko *et al.*, 2011), pAAV-RC2, and pHelper plasmids. The produced AAV vector was purified with AAV purification ViraKit (Virapur, CA, USA) according to the manufacturer's protocol.

PCs could be visually identified by their large cell bodies (Fig. 6A) and thick dendrites, and EGFP fluorescence (Fig. 6B), which preferentially labeled PCs by relatively specific AAV (serotype 2) infection. Each week after seeding, half of the medium was replaced with fresh one with 4 μM cytosine ß-D-arabino-furamoside to inhibit glia proliferation. The cultures were left to mature for four to six weeks before recordings.

***Electrophysiology:*** Electrophysiological experiments were performed following the protocols previously used in our laboratory (Kawaguchi and Sakaba, 2015). In detail: experiments were carried at room temperature (20~24 °C). Unless specified, all whole-cell patch clamp recordings were performed with an amplifier (EPC10, HEKA, Germany) in an extracellular solution containing (in mM) 145 NaCl, 5 KCl, 2 $CaCl_2$, 1 $MgCl_2$, 10 Hepes, and 10 glucose (pH 7.3). In some experiments, 2,3-Dioxo-6-nitro-1,2,3,4-tetrahydrobenzo[f]quinoxaline-7-sulfonamide (NBQX, 10 μM, Tocris Cookson, UK), TEA (2 mM), and tetrodotoxin (TTX, 1 μM, Wako, Japan) were used to inhibit glutamatergic EPSCs, $K^+$ channels, and $Na^+$ channels, respectively.

For PC-PC pair recordings, we identified possible candidates for a presynaptic PC (prPC) via fluorescence, targeting cells with a well-defined axon and clear synaptic contacts on the tentative postsynaptic cell (ptPC). Pairs with relatively short soma-to-soma distance were preferred (~ 200 μm), as well as pairs with low count of synaptic connections, in order to mimic the conditions in slice preparation (Orduz and Llano, 2007). We voltage-clamped the prPC in whole-cell mode using a patch pipette (3 – 5 MΩ) filled with (in mM) 140 D-Glucoronic acid, 7 KCl, 5 EGTA, 10 HEPES, 2 ATP, 0.2 GTP and 155 KOH. Subsequently, we patched the ptPC in whole-cell mode using a patch pipette (3 – 5 MΩ) filled with (in mM) 147 CsCl, 5 EGTA, 10 HEPES, 15 CsOH, 2 ATP, 0.2 GTP, and 2 QX-314. Visualization of the ptPC was done by applying CF568 fluorescent dye (100 μM, Biotium, Hayward, CA). Both cells were clamped at -70 mV. The soma of the prPC was stimulated with a depolarization pulse (-70 mV to 0 mV, 1-2 ms) to induce an escaped AP that propagates to the axon and cause synaptic transmission to the ptPC. Postsynaptic currents (PSCs) were recorded simultaneously. We only accepted the recordings for further analysis in which the ptPC's series resistance was below 25 MΩ and the leak current didn't exceed -200 pA. The paired-pulse ratio (PPR) of PSCs was calculated by dividing the amplitude of the 2nd PSC by that of the 1st one applied at different frequencies (200, 100, 50 and 20 Hz). The 2nd PSC amplitude was obtained by measuring the difference between the peak and the residual current of the 1st PSC which was estimated by extrapolation based on the decay time constant. The paired pulse stimulation was applied every two seconds. The time difference between the onset of presynaptic PC soma stimulation and the visually identified onset of PSC was measured as the onset delay.

For terminal recordings, we selected EGFP-labeled varicosities impinging on the soma

or the proximal dendrites of other PC. We recorded from a terminal using a relatively small patch pipette (16 – 18 MΩ) filled with 147 or 152 (in mM) CsCl, 10 HEPES, 2 ATP, 0.2 GTP, and either 5 or 0.5 EGTA. The $Ca^{2+}$ currents were recorded in the presence of 1 μM TTX and 2 mM TEA to block $Na^+$ and $K^+$ currents, respectively. The effective space clamp at the PC terminal on a PC in culture was estimated by recording capacitive transients in response to a small depolarizing or hyperpolarizing pulse (10 mV) to an axon terminal. Capacitive transients at an axon terminal followed a dual exponential with a fast time constant of 0.15 ± 0.01 ms and a slow time constant of 3.4 ± 0.7 ms (n = 11 cells). Assuming that the terminal was connected to a cylinder shape of axon, the terminal size was estimated to be 1.5 ± 0.3 pF, and a capacitance of the clamped axonal region of 4.6 ± 0.8 pF. These membrane capacitances corresponded to a terminal with 3 μm diameter and an axon of 20 μm lengths inter-connected through a resistance of about 700 MΩ. Considering the relatively sparse synaptic formation between PCs, the area controlled by the voltage command was likely confined to the patched terminal, but not neighbouring ones. This idea was supported by simulation of the electrical circuit consisting of a terminal and an axon. In some experiments, EGTA was replaced with 20 mM BAPTA accompanied with appropriate reduction of CsCl to adjust osmolality. The basal membrane capacitance assuming a single compartment using a patch-clamp amplifier (a terminal plus short axon segment; Cm) was 2-3 pF, and series resistance of the terminal recordings (typically 70 MΩ) was compensated by ~ 30-80 %. Measurements of Cm were carried out using sine + DC technique (Neher and Marty, 1982) implemented on the Patchmaster software (HEKA, Germany). Presynaptic terminals were held at -80 mV and the sine wave (1000 Hz and the peak amplitude of 30 mV) were applied on the holding potential. Because of large conductance changes during the depolarizing pulse, the capacitance jump in response to the depolarizing pulse was usually measured by a difference between 200-300 ms after the pulse and the baseline.

***$Ca^{2+}$ Imaging:*** To record the $Ca^{2+}$ increase in the presynaptic terminals, we applied CF-633 (100 μM, Biotium), and either Oregon Green BAPTA-1 (OGB-1, 200 μM, Invitrogen, Kd = 0.2 μM) or Oregon Green BAPTA-6 (OGB-6, 200 μM, Invitrogen, Kd = 3 μM), both $Ca^{2+}$ sensitive fluorescence dyes, to the soma of a granule cell (GC), an inhibitory interneuron (IN) or a PC through a patch pipette. The dyes were allowed to

diffuse throughout the cell for 25 minutes before recordings started. Axonal varicosities were identified by the CF-633 fluorescence. The $Ca^{2+}$ increase upon an AP (ΔF), which was triggered at the soma by a depolarizing pulse (0 mV, 2 ms), was detected as fluorescence increase of OGB-1/OGB-6, quantified as ΔF/F. To record the fluorescence changes upon the stimulation, we used a monochrometer with a wavelength set at 470-480 nm. The emission between 510-550 nm was detected by a Zyla sCMOS camera (Andor). The obtained images of PC axon terminals were analyzed with SOLIS (Andor) or Image J (NIH). Five to twenty trails were performed per cell, with one-minute interval in between.

By using ΔF/F, we estimated the increase in $[Ca^{2+}]_i$ upon AP stimulation in the following way: (1) Schmidt *et al.* (2003) have carefully made a calibration of OGB-1 at Purkinje cells, and according to this, ΔF/F of 0.1 should be comparable to 10 nM. (2) From the known Kd of OGB-1 and OGB-6 and basal fluorescence of 20% of the maximal response, we could roughly estimate that the $[Ca^{2+}]_i$ increase is 10-20 nM.

***Statistics:*** Data are presented as mean ± s.e.m. Statistical significance was assessed by paired t-test, unpaired Students' t-test, Mann-Whitney U test or ANOVA.

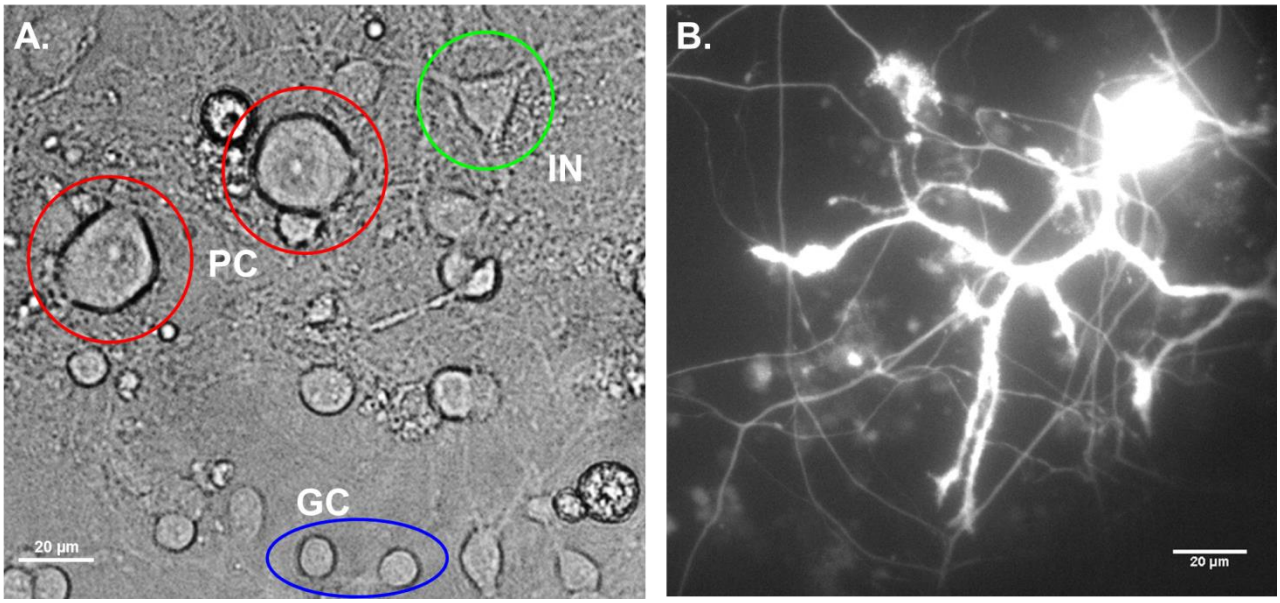


**Figure 6. Cerebellar culture.** A. Purkinje cells (PC, circled in red) can be visually identified by their large size and round/oval soma from other kind of cells found in the culture, like granule cells (GC, circled in blue) and interneurons (IN, circled in green).

B. PCs could also be identified by EGFP fluorescence, which preferentially labeled PCs. The thick dendritic tree with abundant spines is a characteristic morphological feature of PCs.

# Chapter 3. Results

## 3.1. PPF of synaptic transmission at PC–PC synapses in culture

We first tested whether short-term facilitation takes place at inhibitory GABAergic synapses between cultured PCs as in slice preparation (Orduz and Llano, 2007). Culturing cells may alter functional properties of PCs, and this may affect the facilitation property at this synapse.

PCs were sparsely labelled with EGFP fluorescence using AAV vector (Kaneko *et al.* 2011), which allowed us to identify a synaptically connected pair of PCs (Fig. 7*A*). PCs tend to form synapses on a DCN neuron (Kawaguchi and Sakaba, 2015) and synaptically connected PC–PC pairs were rarely found in culture. We performed whole-cell patch clamp recordings from a pair of PCs that were located relatively near, as in slice preparation (Orduz and Llano, 2007). To improve visualization of the pair, we preferred pairs of PCs in which only the presynaptic PC was labeled by EGFP. The postsynaptic PC, on the other hand, was visualized by fluorescence using CF568 or CF633 applied through a recording patch pipette. The distance from the axon hillock to the first branching point of the axon collateral was 130 ± 20 µm, and the distance between the presynaptic PC soma and the closest synapse was 530 ± 99 µm ($n$ = 8 pairs). The presynaptic PC made approximately six synaptic contacts on average (6.43 ± 0.87) on the soma or dendrites of the postsynaptic PC. Synaptic contacts were identified visually. Only those overlapping the postsynaptic cell and with oval morphology (1-3 µm in size) were counted. Although varicosity-like morphology does not guarantee synaptic contacts, varicosities on other PCs usually showed $Ca^{2+}$ influx upon AP stimulation (see below), which led us to conclude that they are classified as a terminal. Both pre- and postsynaptic PCs were voltage clamped at −70 mV. Paired pulse stimulation consisting of two depolarization pulses (to 0 mV, for 2 ms) was applied to the presynaptic PC soma (to elicit APs) at different intervals (5, 10, 20 and 50 ms) and synaptic transmission was recorded from the postsynaptic PC. The PSC was recorded as inward currents because of a high concentration of internal $Cl^-$ (to improve signal-to-noise ratio), and had an average amplitude of 409 ± 153 pA ($n$ = 8 pairs with six synaptic contacts on average), onset delay of 2.6 ± 0.2 ms, 10–90% rise time of 2.0 ± 0.2 ms and half-height width of 15 ± 2 ms. As shown in Fig. 7*B*, the

amplitude of the second PSC was larger than that of the first one, and the extent of facilitation depended on the stimulation interval (50 ms, 107 ± 2%; 20 ms, 122 ± 4%; 10 ms, 134 ± 6%; 5 ms, 150 ± 9%; $n$ = 6–7 cells) (Fig. 7*C* and *D*). The time course of PPF was comparable to that reported in acute slice preparation (Orduz and Llano, 2007). Thus, the facilitation property of GABAergic synapses between PCs is preserved in the dissociated culture.

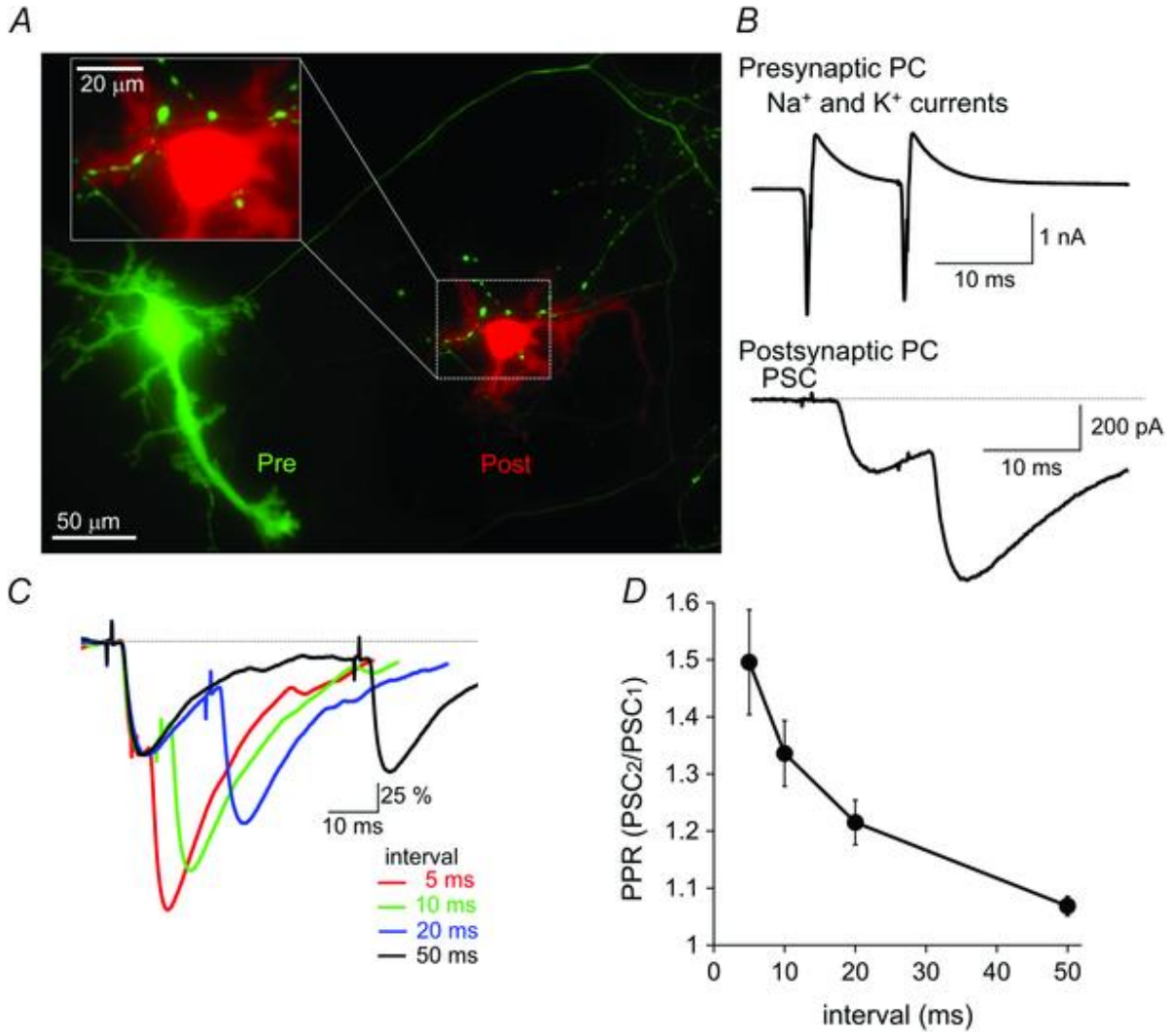


**Figure 7. PPF of synaptic transmission at the cultured PC–PC synapse.** *A*, fluorescence image of a synaptically-connected PC–PC pair. Green: a presynaptic PC expressing EGFP. Red: a postsynaptic PC visualized by CF633 applied through a patch pipette (removed for the image acquisition). To show several synapses around the postsynaptic PC soma and proximal dendrites, the area surrounded by a white rectangle is presented as an enlarged image. *B*, representative traces of presynaptic $Na^+$and $K^+$ currents and PSCs upon paired pulse stimulation at a 10 ms interval (depolarization pulses to 0 mV for 2 ms). Presynaptic currents through voltage-dependent channels were isolated by subtracting the 7-fold capacitive currents upon the 10 mV depolarization pulse. *C*, normalized PSC traces upon paired-pulse

stimulation at 5, 10, 20 or 50 ms intervals. *D*, averaged ratio of PSC amplitudes (PSC2/PSC1) is plotted against the interval of paired pulse stimulation ($n$ = 6–7 pairs).

## 3.2. Short-term facilitation of $Ca^{2+}$ currents in a PC terminal

To study the mechanism underlying short-term facilitation at PC–PC synapses, we performed direct whole-cell voltage patch-clamp recordings from a presynaptic PC terminal (1–3 µm in diameter) impinging on the soma or proximal dendrite of a PC, and the impinged postsynaptic PC (Fig. 8*A*). The PC terminal was labeled with EGFP to increase visibility and aid patch-clamping. We first recorded the presynaptic $Ca^{2+}$ currents through voltage-gated $Ca^{2+}$ channels upon stimulation and the resultant postsynaptic response. To mimic the physiological conditions of synaptic transmission, in which a presynaptic terminal is activated by the arrival of an AP, we did not stimulate the presynaptic button with a simple square depolarization pulse. Instead, stimulation was done by applying a voltage command with an AP waveform that was previously recorded from a PC terminal on a DCN neuron in a previous study (Kawaguchi and Sakaba, 2015), which was similar to the AP waveform recorded from a PC terminal on a PC (Fig. 8*B*). To restrict propagation of APs to the patched terminal, we patch-clamp recorded from a relatively isolated terminal in the presence of 1 µM TTX, a selective $Na^+$ channel blocker.

Paired recordings from a PC axon terminal and a postsynaptic PC soma showed that a single presynaptic AP commands evoked a PSC with mean amplitude of 116 ± 32 pA ($n$ = 10 pairs). To study the relationship between the stimulating AP command, the presynaptic $Ca^{2+}$ currents and the PSCs, we gradually changed the peak amplitude of the AP command. As it became larger in amplitude, the $Ca^{2+}$ current almost linearly increased (Fig. 8*C,* bottom left). On the other hand, the PSC amplitude changed supralinearly, and showed a 4–5th power dependency on the $Ca^{2+}$ current amplitude (Fig. 8*C,* top right). This supralinearity is similar to that observed in the $Ca_{free}$ – NT released relationship (Katz and Miledi, 1968; see Section 1.1), which suggests that the facilitation of the PC – PC synapse may be primarily due to presynaptic processes.

In order to quantify the transmission between the PCs, we recorded miniature PSCs in the postsynaptic cell. First, because PCs receive inputs from many neurons, it was necessary to isolate the miniature PCSs only arisen from a given synapse to avoid

contamination. This was done by analyzing asynchronous events following a strong pulse to the presynaptic terminal. A strong depolarization pulse (5 ms in duration) greatly increases $Ca_{free}$ in the presynaptic terminal, causing an increase in the release probability of the synaptic vesicles. Miniature PSCs could then be observed as asynchronous releases after a strong square pulse to the terminal, with a mean amplitude of 52 ± 3 pA ($n$ = 6 pairs) (Fig. 8*D*). Compared this value with the mean amplitude of PSC upon AP stimulation (116 pA), we conclude that a few synaptic vesicles are exocytosed upon an AP command, which is similar to a previous study at the connection between PC and the DCN neuron (Kawaguchi and Sakaba, 2015). In addition, the amplitude of PSCs was in a reasonable range considering that a PC pair showing the mean PSC amplitude (409 pA) under somatic paired recordings had approximately six synaptic connections located at various postsynaptic compartments morphologically (Fig. 7). Taken all of these observations together, the AP voltage command to the PC axon terminal causes synaptic transmission compatible with the physiologically evoked one.

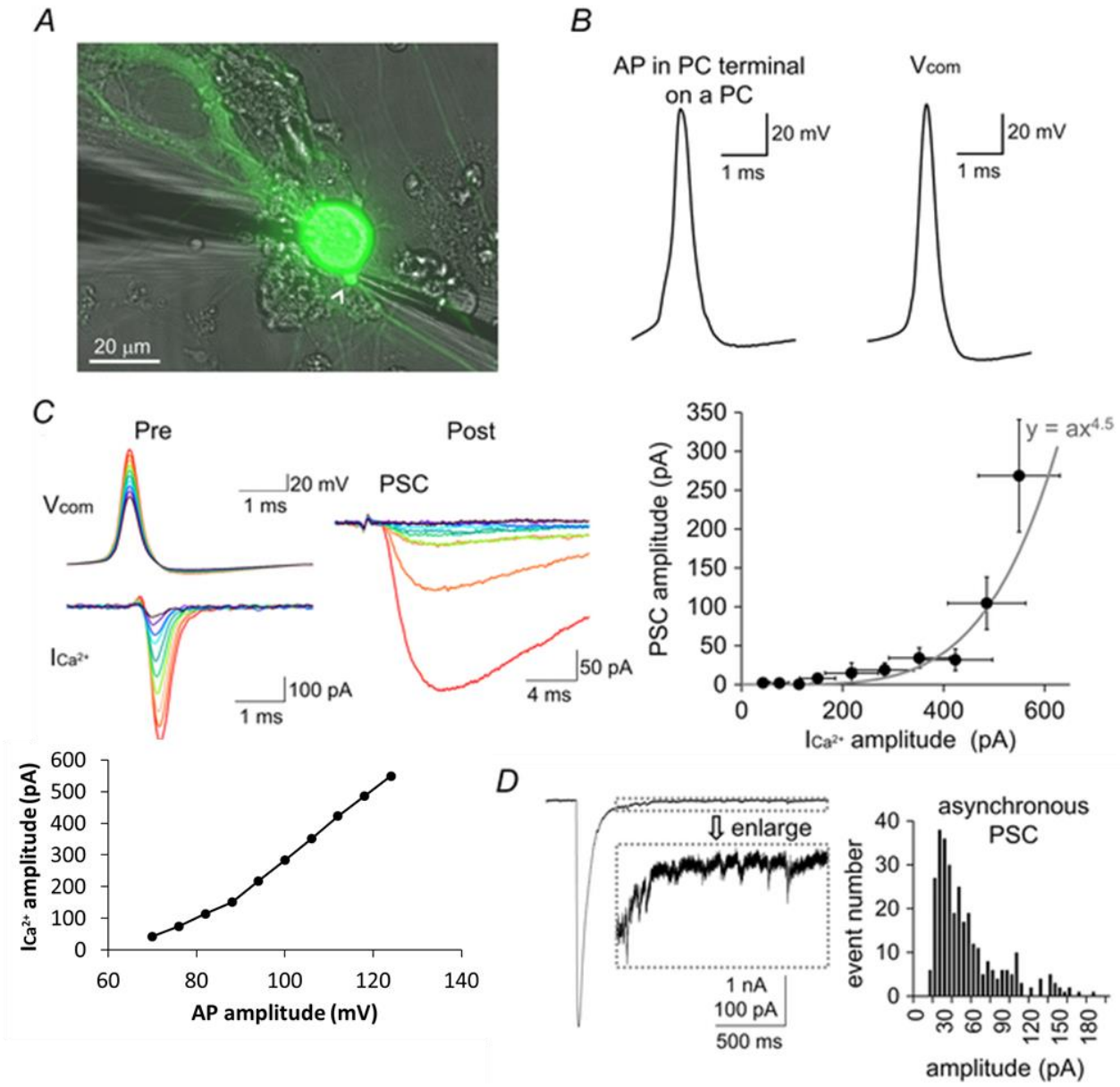


**Figure 8. PC–PC synaptic transmission upon an AP voltage command at a terminal.** *A*, representative image for paired recordings from the presynaptic PC terminal (highlighted by a white arrowhead) and the postsynaptic PC soma. Both pre- and postsynaptic PCs are EGFP-positive in this case. *B*, AP waveform recorded from a PC terminal impinging on a PC (left) and the AP waveform used for voltage command in the present study that was recorded from a PC terminal on a DCN (right). *C*, top left: representative traces of different amplitudes of AP commands ($V_{com}$), the $Ca^{2+}$ currents ($I_{Ca^{2+}}$) in a presynaptic PC terminal and the PSCs simultaneously recorded from the postsynaptic PC. Top right: PSC amplitudes upon various amplitudes of AP commands were plotted against the $I_{Ca^{2+}}$ amplitudes. The grey line represents the 4.5th power relationship between *x*- and *y*-axis. Bottom left: Peak amplitude of the $I_{Ca^{2+}}$ against the amplitude of the stimulating AP (in percentage). *D*, left: a representative trace of PSC evoked by the 5 ms depolarization pulse to 0 mV in the presynaptic terminal. For hundreds of milliseconds after the evoked PSC, asynchronous events could be observed. These events were used for sampling mPSCs because this is the most reliable way of

collecting miniature events from a given presynaptic PC terminal. Right: amplitude histogram of asynchronous PSCs. Pooled data from six cells are shown.

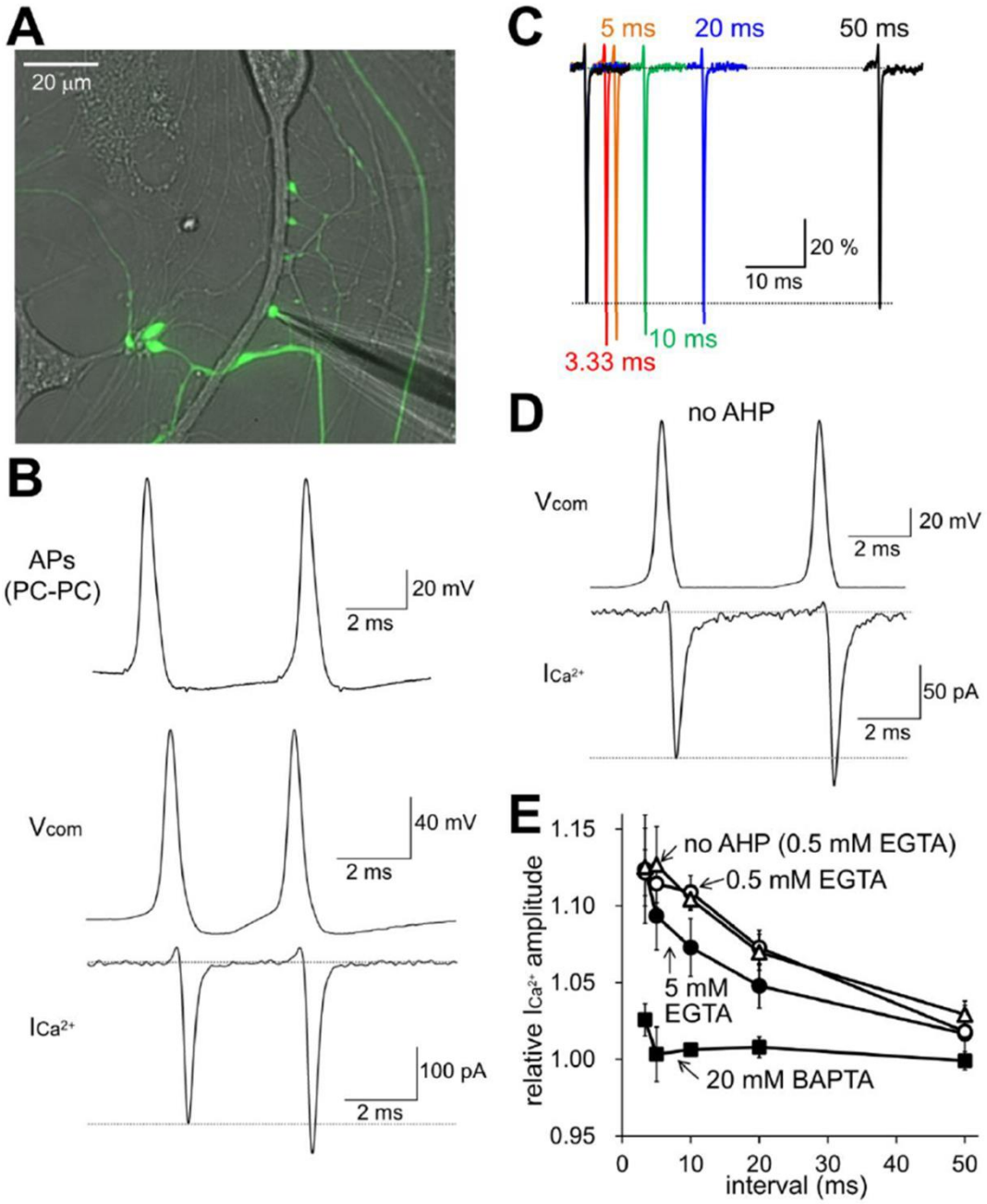


**Figure 9. $Ca^{2+}$-dependent facilitation of presynaptic $Ca^{2+}$ currents at PC–PC synapses.** *A*, image of direct patch clamp recording from an EGFP-positive axon terminal on a proximal dendrite of another PC. *B*, pair of APs recorded from a PC terminal on a PC (top), representative traces of paired-pulse voltage commands with an AP waveform (middle, $V_{com}$) and the resultant $Ca^{2+}$currents (bottom, $I_{Ca^{2+}}$). *C*, normalized $Ca^{2+}$ currents upon paired-pulse AP commands at 3.33, 5, 10, 20 or 50 ms interval. The dotted line represents the average peak amplitude of the first $Ca^{2+}$ current. *D*, representative traces of the paired-pulse voltage command with an identical AP waveform without AHP and the resultant $Ca^{2+}$ currents. *E*, averaged $Ca^{2+}$ current facilitation upon various intervals of paired-pulse AP waveforms in the presence of 0.5

or 5 mM EGTA or of 20 mM BAPTA. The data obtained without AHP of the AP waveform in the presence of 0.5 mM EGTA are also shown (no AHP) [$n = 4$ (0.5 mM EGTA, 5 mM EGTA and 20 mM BAPTA); $n = 5$ (no AHP)].

To examine whether the $Ca^{2+}$ currents are modulated during high-frequency AP arrivals, more specifically, whether the currents exhibit short-term plasticity, we stimulated the presynaptic terminal by paired pulses of the AP command (Fig. 9*A*). As shown in Fig. 9*B*, the waveform of an AP pair recorded from a PC terminal upon somatic high frequency stimulation showed afterhyperpolarization (AHP) between two APs. Therefore, we used a similar voltage command with AHP for the paired pulse stimulation of the PC terminal, unless otherwise stated.

The amplitude of $Ca^{2+}$ current upon the second AP waveform was larger than that upon the first one, showing PPF dependent on the stimulation interval (3.33 ms, 112 ± 2%; 5 ms, 111 ± 2%; 10 ms, 111 ± 1%; 20 ms, 107 ± 1%; 50 ms, 102 ± 2%) (Fig. 9*B*, *C* and *E*). There are two possible candidate mechanisms for the $Ca^{2+}$ current facilitation upon the paired-pulse stimulation of the AP command. One is that AHP between the first and the second AP commands may recover some fraction of voltage-gated $Ca^{2+}$ channels from inactivation at resting membrane potential (Brachaw *et al.* 1997), leading to increased availability of $Ca^{2+}$ channels at the second stimulation. To test this possibility, we omitted AHP between two AP commands and measured the PPF of $Ca^{2+}$ currents (Fig. 9*D*). As shown in Fig. 9*D* and *E*, the PPF of $Ca^{2+}$ currents without AHP was similar to that observed in the presence of AHP (3.33 ms, 113 ± 3%; 5 ms, 113 ± 2%; 10 ms, 109 ± 1%; 20 ms, 107 ± 1%; 50 ms, 103 ± 1%). The other candidate mechanism is the $Ca^{2+}$-dependent facilitation of $Ca^{2+}$ currents, which is caused by direct modulation of voltage-gated $Ca^{2+}$channels by $Ca^{2+}$-binding proteins such as calmodulin (CaM) and neuronal $Ca^{2+}$ sensor (Catterall and Few, 2008; Ben-Johny and Yue, 2014). To test this possibility, the PPF of $Ca^{2+}$ current was measured in the presence of higher concentration of $Ca^{2+}$ chelator in the intracellular solution. Increase of intracellular concentration of EGTA (from 0.5 mM to 5 mM) did not suppress the PPF of $Ca^{2+}$ current at short intervals but accelerated the decay of the PPF of $Ca^{2+}$ current (3.33 ms, 112 ± 4%; 5 ms, 109 ± 2%; 10 ms, 107 ± 2%; 20 ms, 105 ± 1%; 50 ms, 102 ± 0%) (Fig. 9*E*). Application of BAPTA (20 mM), a $Ca^{2+}$ chelator with a similar $Ca^{2+}$ affinity (Kd) as EGTA but with much faster $Ca^{2+}$ binding kinetics,

was necessary to abolish completely the $Ca^{2+}$ current facilitation (3.33 ms, 103 ± 1%; 5 ms, 100 ± 2%; 10 ms, 101 ± 0%; 20 ms, 101 ± 1%; 50 ms, 100 ± 1%) (Fig. 9*E*). Taking all of these results together, it was suggested that the $Ca^{2+}$ current through voltage-gated $Ca^{2+}$ channels is facilitated upon high-frequency stimulation depending on the increase in intracellular $Ca^{2+}$ concentration ($[Ca^{2+}]_i$).

## 3.3. PPF of synaptic transmission is determined by that of $Ca^{2+}$ currents

Taking into consideration that transmitter release is supra-linearly dependent on the $[Ca^{2+}]_i$ (Fig. 8*C*), the PPF of $Ca^{2+}$ currents might be a powerful mechanism leading to the short-term facilitation of synaptic transmission. To study the quantitative relationship between the PPF of $Ca^{2+}$currents and that of synaptic transmission, we performed paired recordings from a presynaptic PC axon terminal and a postsynaptic PC soma. Paired-pulse AP waveforms with different intervals caused facilitation in both the presynaptic $Ca^{2+}$ current amplitude (3.33 ms, 116 ± 2%; 5 ms, 114 ± 2%; 10 ms, 112 ± 2%; 20 ms, 110 ± 2%; 50 ms, 103 ± 2%) and PSCs (3.33 ms, 202 ± 14%; 5 ms, 209 ± 8%; 10 ms, 174 ± 3%; 20 ms, 170 ± 20%; 50 ms, 108 ± 14%) (Fig. 10*A*–*C*). The facilitation of PSCs could be fitted to the 4–5th power of that of $Ca^{2+}$ currents (Fig. 10*B* and *C*). Least square method showed the value of 4.5-5, and because the data scatter to some extent and the power is estimated to be 4.5 from previous studies (Schneggenburger and Neher, 2000), we used the value of 4.5. When the decay from $Ca^{2+}$ current facilitation was accelerated by the presence of 5 mM intracellular EGTA (3.33 ms, 114 ± 1%; 5 ms, 112 ± 1%; 10 ms, 109 ± 1%; 20 ms, 105 ± 1%; 50 ms, 102 ± 1%), the PPF of PSC also recovered faster (3.33 ms, 198 ± 14%; 5 ms, 170 ± 9%; 10 ms, 151 ± 12%; 20 ms, 118 ± 16%; 50 ms, 99 ± 11%), showing 4–5th power dependence of the PSC facilitation on the $Ca^{2+}$ current facilitation (Fig. 10*C*). Thus, the PPF of PSCs was tightly correlated with that of the $Ca^{2+}$ currents. The time course of the PSC facilitation observed by paired terminal-soma recordings in the presence of 5 mM rather than 0.5 mM EGTA was similar to that observed under paired soma–soma recordings from synaptically-connected PCs (Fig. 7). Thus, the strong $Ca^{2+}$ buffering capacity of PC terminals containing calbindin and parvalbumin (Bornschein *et al.* 2013) might be similar to the situation containing a millimolar-order of EGTA. It is important to note that due to whole-cell dialysis, endogenous $Ca^{2+}$

buffers might have been washed out from the terminal.

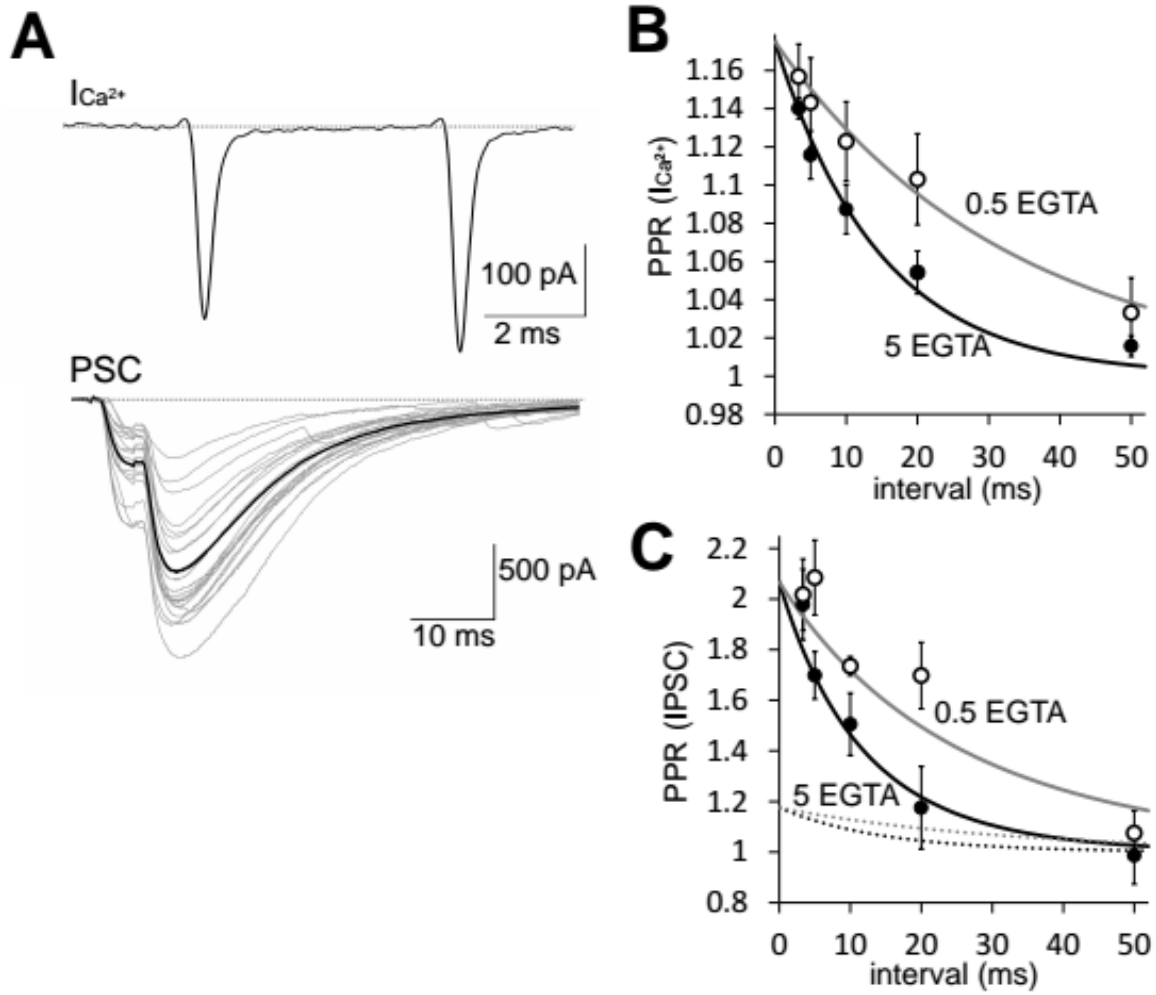


**Figure 10. Tight coupling of $Ca^{2+}$ current facilitation and synaptic facilitation at PC–PC synapses.** *A*, representative traces of $I_{Ca^{2+}}$ (average of 20 traces) and PSCs upon paired pulse voltage commands consisting of an identical AP waveform. Black PSC trace is the average of 20 PSC traces shown in grey. *B* and *C*, averaged PPR of $I_{Ca^{2+}}$ (*B*) and that of PSC (*C*) in the presence of intracellular 0.5 or 5 mM of EGTA are plotted against the interstimulus interval. Grey or black continuous lines in (*C*) are the 4.5th power of $I_{Ca^{2+}}$ (shown as dotted lines, which are same as continuous lines in *B*) [$n$ = 6 pairs (5 mM EGTA); $n$ = 4 pairs) (0.5 mM EGTA)].

To examine the causal relationship between the PPF of $Ca^{2+}$ current and that of PSC, it was necessary to study the PSCs in the absence of $Ca^{2+}$ current facilitation, and observe whether the PPF of PSCs remained unchanged or not. For this, following the previous results (Fig 6C) that show linear dependency of the $Ca^{2+}$ current amplitude on the AP voltage command amplitude and the amplitude of $Ca^{2+}$ currents, we next

varied the amplitude of $Ca^{2+}$ currents during the second AP voltage command by systematically altering the peak amplitude of the second AP (to 1.05, 1, 0.95, 0.9 or 0.85 times the first AP) (Fig. 11*A*). As the amplitude of the second AP command decreased, that of the second $Ca^{2+}$ current peak was also decreased (1.05AP, 123 ± 3%; 1AP, 113 ± 1%; 0.95AP, 104 ± 1%; 0.9AP, 93 ± 2%; 0.85AP, 80 ± 3%) (Fig. 11*A* and *C*). As a result of the decreased $Ca^{2+}$ current, PPR of the PSCs changed into from PPF to paired-pulse depression (1.05AP, 236 ± 31%; 1AP, 175 ± 27%; 0.95AP, 136 ± 15%; 0.9AP, 83 ± 15%; 0.85AP, 64 ± 13%)(Fig. 11*B* and *C*).

We plotted the paired-pulse ratio (PPR) of the PSCs against that of $Ca^{2+}$ currents and observed that their relation matched the 4-5th power dependence (Fig. 11*C*). Technically, it is difficult to set the PPR of $Ca^{2+}$ currents exactly to 1. However, in a fitted curve to the data, when the facilitation of $Ca^{2+}$ currents is suppressed (1 in the horizontal axis), so does the facilitation of PSCs gets suppressed (1 in the vertical axis). This result, together with that shown in Fig. 10, indicates that the paired pulse ratio of PSCs critically depends on the 4–5th power of $Ca^{2+}$ currents, and thus, it appears that the PPF of synaptic transmission is predominantly brought about by the PPF of $Ca^{2+}$ currents at the PC–PC synapses.

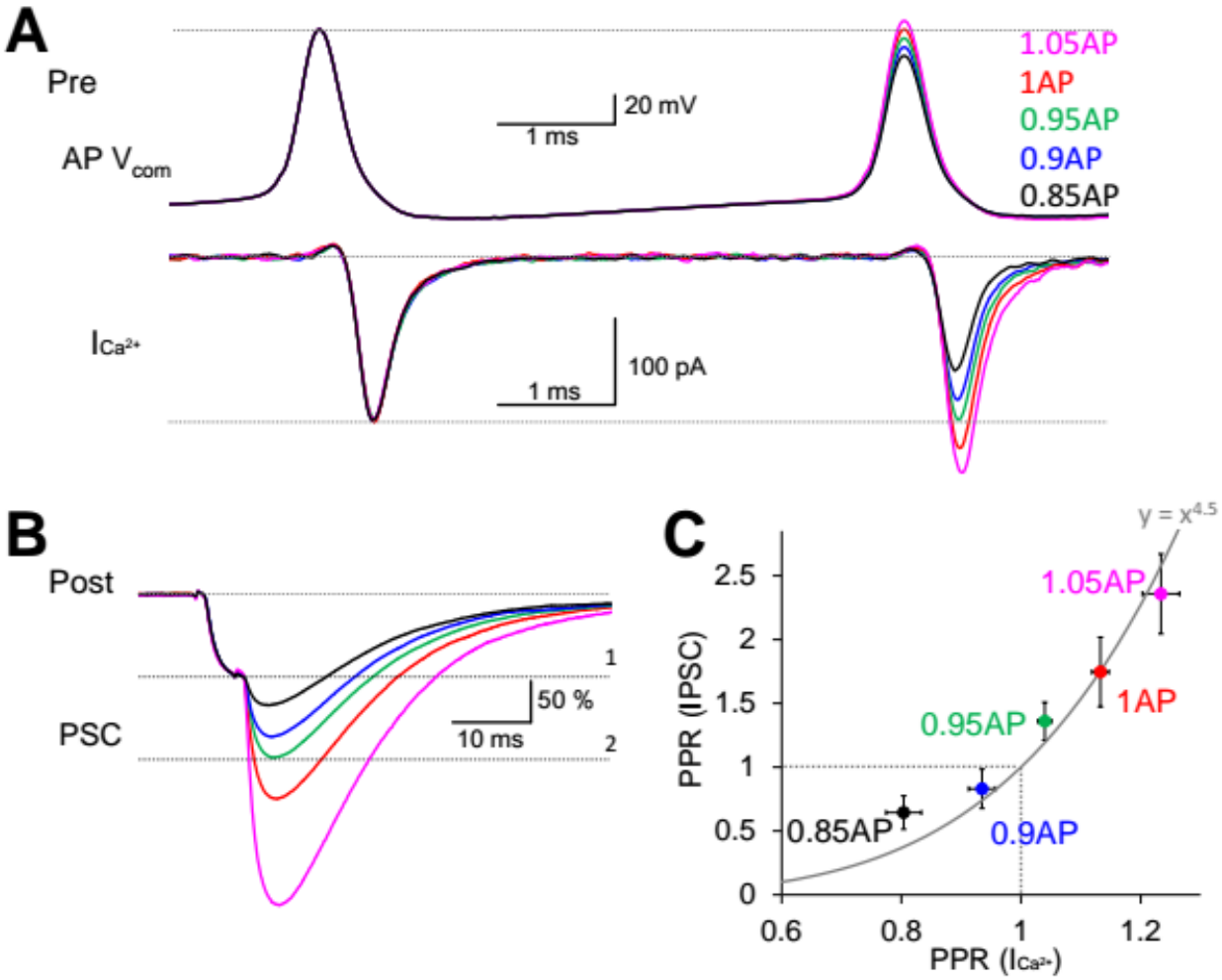


**Figure 11. $I_{Ca^{2+}}$ facilitation determines the synaptic facilitation.** *A* and *B*, representative traces of voltage commands consisting of paired-pulse AP waveforms ($V_{com}$) and the $Ca^{2+}$ currents ($I_{Ca^{2+}}$) in a presynaptic PC terminal (*A*) and of PSCs (*B*). The second AP amplitude was changed (1.05, 1, 0.95, 0.9 or 0.85 times that of the first) to alter the second $Ca^{2+}$ current amplitude. The PSC amplitudes were normalized to the first one for clarity. *C*, the averaged PPR of PSCs was plotted against that of $I_{Ca^{2+}}$. The data were obtained from the experiments shown in (*A*) and (*B*) ($n$ = 6 pairs).

## 3.4. Marginal residual $Ca^{2+}$ in a PC terminal

The above results precluded major contribution of other mechanisms of facilitation, such as the residual $Ca^{2+}$ hypothesis, which suggested that temporal summation of $[Ca^{2+}]_i$ during paired AP arrivals increases the transmitter release probability (Katz and Miledi, 1968). To test this issue further, we attempted to study the residual $Ca^{2+}$ at the PC synaptic terminal, the other major mechanism that may underlie facilitation at this synapse. To do this, we first selected PCs that did not expressed EGFP and

performed $Ca^{2+}$ imaging. We applied $Ca^{2+}$-sensitive indicators OGB-1 (200 μM, $K_d$ = 0.2 μM) or OGB-6 (200 μM, $K_d$ = 3 μM), together with CF633 into the soma through a patch pipette (Fig. 12*A*). CF633 dye was added to aid identifying axonal varicosities, as the large amount of endogenous $Ca^{2+}$ buffers in PCs makes the $Ca^{2+}$-indicators to have a low signal-to-noise ratio at basal $Ca^{2+}$. Similar experiments were also conducted in two other cells present in our cultures, granule cells (GC) and inhibitory interneurons (IN) to serve as control.

Because of the low temporal resolution of the OGB indicators, it was not possible to perform a paired-pulse stimulation protocol. Instead, we recorded the increase in fluorescence at synaptic varicosities as a measure of $Ca_{free}$ upon single AP stimulation. By knowing the relative increase in fluorescence upon stimulation, and by knowing the local $Ca^{2+}$ concentration at the release zone, it is possible to calculate the increased NT released due to the contribution of the increased residual $Ca_{free}$.

After 25 min of dye diffusion, we evoked an AP by applying a single depolarization pulse to the PC soma (to 0 mV, 2 ms) and the fluorescence changes in the axonal varicosities were recorded. The $Ca^{2+}$ influx into the varicosity resulted in the increase in fluorescence signal of OGB-1 or OGB-6, and the relative fluorescence increase ($\Delta F/F$) reflected the amplitude of $Ca^{2+}$ increases. The $\Delta F/F$ upon a single AP was very small in a PC terminal (OGB-1, 0.11 ± 0.01) compared to the varicosities of an interneuron (IN, 0.38 ± 0.12) or a granule cell (GC, 0.45 ± 0.16). An IN is known to express parvalbumin but not calbindin, whereas a GC lacks both but expresses calretinin (Bastianelli, 2003). The $\Delta F/F$ was extremely small in a PC terminal when using OGB-6 (PC: 0.03 ± 0.01; IN: 0.19 ± 0.05; GC: 0.23 ± 0.03) (Fig. 12*B* and *C*). Thus, the residual $[Ca^{2+}]_i$ increase is tiny in a PC terminal compared to axon terminals of an IN or a GC. We estimated that the change of OGB-1 and OGB-6 fluorescence upon a single AP in a PC terminal corresponded to an~10–20 nM of $[Ca^{2+}]_i$ increase, which is similar to the value estimated in previous slice studies (Schmidt *et al.* 2003; Orduz and Llano, 2007). A high expression level of $Ca^{2+}$ buffer proteins, calbindin and parvalbumin, probably suppresses the residual $[Ca^{2+}]_i$ increase (Bornschein *et al.* 2013). Considering a previous estimate of the local $[Ca^{2+}]_i$ during a single AP as 5–10 μM in a PC terminal (Kawaguchi and Sakaba, 2015), the residual $Ca^{2+}$ increase by 20 nM is estimated to increase the transmitter release by ~1% assuming 4–5th power $Ca^{2+}$ dependence. Thus, in line with the idea that the PPF of the PSCs is

predominantly mediated by that of $Ca^{2+}$ currents, the temporal summation of residual $Ca^{2+}$ probably plays no major role in the PPF of synaptic transmission at PC–PC synapses.

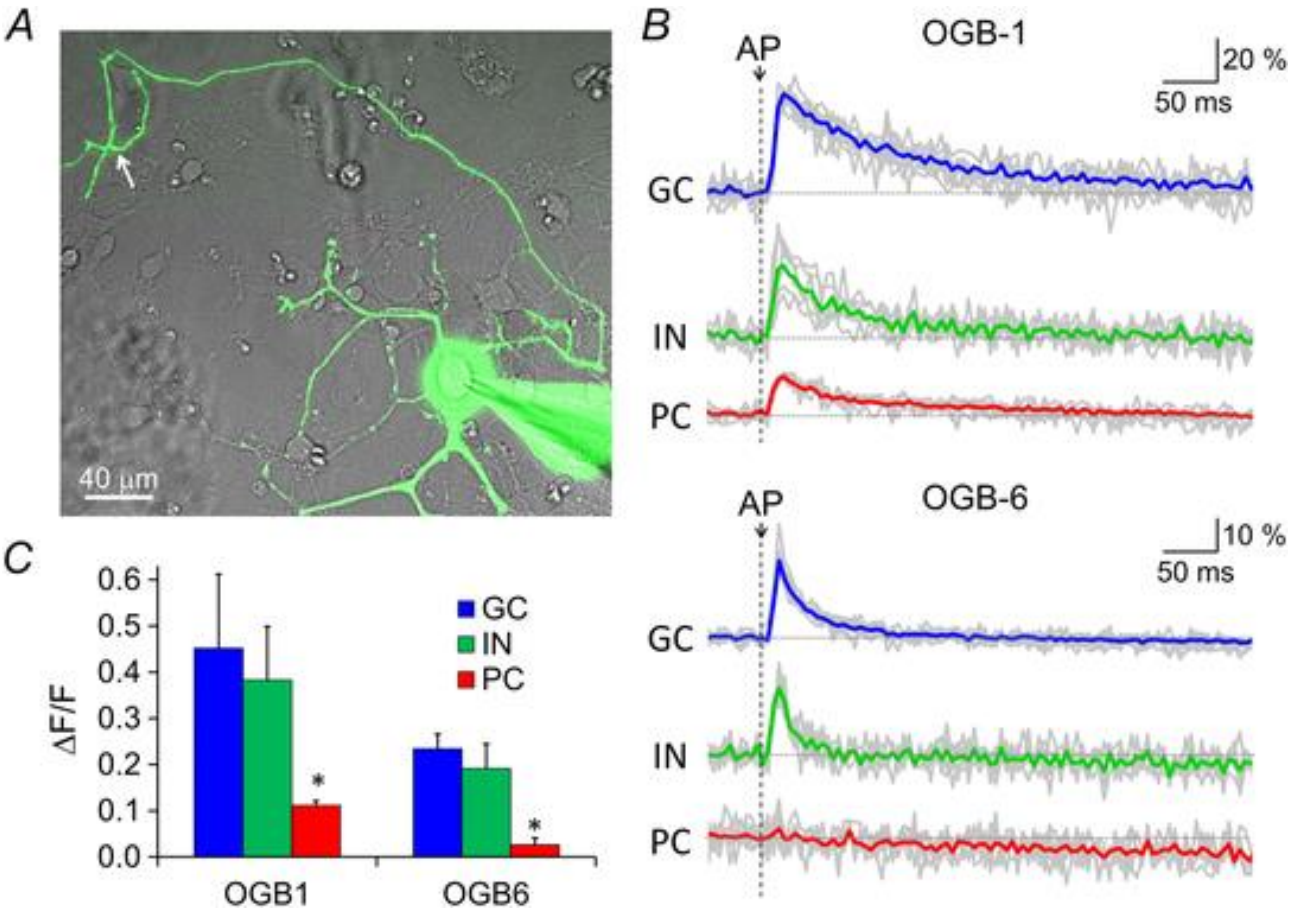


**Figure 12. Residual $Ca^{2+}$ increase at PC terminals.** *A*, representative fluorescence image of a PC loaded with 200 μM OGB-1. At an axon varicosity (highlighted by a white arrow), fluorescence change was measured before and after the action potential evoked at the soma. *B*, time courses of normalized fluorescence intensity change of OGB-1 or OGB-6 recorded from an axon varicosity from a PC, an interneuron (IN) or a granule cell (GC). Representative traces for each condition are also shown in grey. *C*, $\Delta F/F$ upon single AP in a GC ($n = 6$ cells for OGB-1 and 8 for OGB-6), IN ($n = 5$ cells for OGB-1 and 6 for OGB-6) or PC ($n = 7$ cells for OGB-1 and 5 for OGB-6). $^*P < 0.05$.

## 3.5. Release properties of PC axon terminals on a PC are similar to those on a DCN neuron

The above results indicated that the facilitative property of PC synapses on another PC is predominantly mediated by $Ca^{2+}$-dependent facilitation of $Ca^{2+}$ currents through voltage-gated $Ca^{2+}$ channels. On the other hand, PC synapses on a DCN neuron show

depression upon high-frequency stimulation (Telgkamp and Raman, 2002) as a result of AP attenuation around terminals (Kawaguchi and Sakaba, 2015). To study the mechanism underlying the target-dependent opposite forms of short-term synaptic plasticity, we next examined whether the facilitation of $Ca^{2+}$ currents and the resultant enhancement of transmitter release is a unique mechanism of PC synapses on another PC but not on DCN neurons. As shown in Fig. 13, cultured PC axons preferentially formed high density of synapses around a type of neuron, which is estimated to be a potential DCN neuron based on morphology, electrophysiological properties and molecular marker expression (Kawaguchi and Sakaba, 2015). We performed paired whole-cell recordings from the presynaptic PC axon terminal and the postsynaptic DCN cell. Similar to PC–PC synapses, paired-pulse voltage commands of an AP waveform to the presynaptic terminal caused facilitation of presynaptic $Ca^{2+}$ currents (3.33 ms interval, 114 ± 1%; 5 ms, 113 ± 2%; 10 ms, 114 ± 1%; 20 ms, 107 ± 2%; 50 ms, 103 ± 2%) (Fig. 13*B* and *C*). Consequently, the synaptic transmission also exhibited PPF rather than depression (3.33 ms, 177 ± 9%; 5 ms, 181 ± 10%; 10 ms, 182 ± 26%; 20 ms, 144 ± 9%; 50 ms, 123 ± 9%) (Fig. 13*B* and *D*). Interestingly, the extents of facilitation of $Ca^{2+}$ currents and that of PSCs were similar to those observed at PC–PC synapses, and the relationship between facilitation of $Ca^{2+}$ currents and that of PSCs also showed the 4–5th power dependence. In addition, the $Ca^{2+}$ current facilitation at PC synapses on DCN cells was shortened by increasing the EGTA concentration to 5 mM (3.33 ms interval, 111 ± 3%; 5 ms, 110 ± 2%; 10 ms, 108 ± 2%; 20 ms, 104 ± 2%; 50 ms, 100 ± 1%), as for PC–PC synapses (Fig. 13*C*). Consequently, the PPF of the PSCs was also shortened (3.33 ms, 164 ± 13%; 5 ms, 149 ± 21%; 10 ms, 133 ± 15%; 20 ms, 117 ± 11%; 50 ms, 91 ± 5%) (Fig. 13*D*). Thus, the $Ca^{2+}$-dependent facilitation of $Ca^{2+}$ currents causing short-term facilitation is a common feature in PC axon terminals, irrespective of the target neuron type, as long as identical APs are elicited. Indeed, a recent study by Kawaguchi and Sakaba (Kawaguchi and Sakaba, 2015) has demonstrated that the attenuation of the AP conduction around the presynaptic terminal is a major mechanism of synaptic depression at the synapse between the PC and the DCN neuron both in culture and slice preparation.

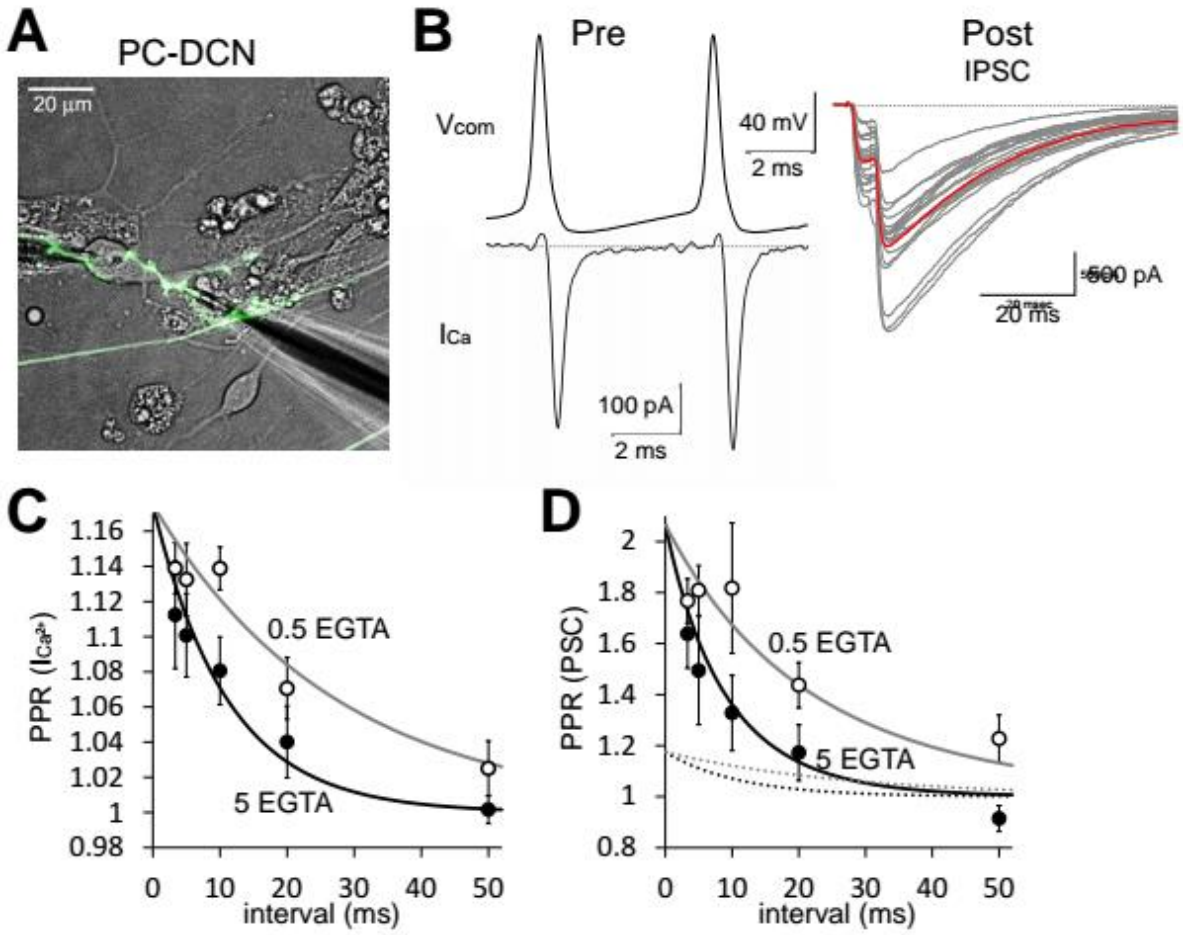


**Figure 13. $Ca^{2+}$-dependent PPF of $Ca^{2+}$ currents and PSCs at PC–DCN synapses.** *A*, representative image for paired recordings from a presynaptic PC terminal and a postsynaptic DCN neuron. *B*, representative traces of the paired-pulse AP command ($V_{com}$) and the $Ca^{2+}$ currents ($I_{Ca^{2+}}$) in a presynaptic PC terminal (top) and the PSCs simultaneously recorded from a postsynaptic DCN neuron (bottom). Red trace is the averaged PSC from 20 PSC traces (grey). *C* and *D*, averaged PPR of $I_{Ca^{2+}}$ (*C*) and that of PSC (*D*) in the presence of intracellular 0.5 or 5 mM of EGTA are plotted against the interstimulus interval. Black or grey lines in (*D*) are the 4.5th power of $I_{Ca^{2+}}$ (shown as dotted lines, which is same as the continuous lines in *C*) ($n$ = 5 and 6 for 5 and 0.5 mM EGTA, respectively).

In addition, the size of total readily releasable pool of synaptic vesicles was also similar when measured by a change of membrane capacitance (Cm). During exocytosis of synaptic vesicles, the vesicles fusion with the terminal membrane increases the total surface area and thus the capacitance. $Ca^{2+}$ influx into the PC terminal caused by different durations (1–50 ms) of square depolarization pulses increased Cm, reflecting exocytosis of synaptic vesicles (Fig. 14). The amplitude of Cm increase could be fitted by a single exponential curve, suggesting a homogenous pool of the readily

releasable vesicles. The PC–PC presynaptic terminal showed 83 ± 24 fF increase upon the 50 ms depolarization pulse, whereas the PC–DCN terminal showed 93 ± 27 fF ($P > 0.39$). Thus, assuming the Cm of single synaptic vesicle to be ~70 aF (Kawaguchi and Sakaba, 2015), ~1000 releasable synaptic vesicles are contained in each terminal. Consistent with the previous data (Kawaguchi and Sakaba, 2015), the Cm increase was not suppressed by increasing the intracellular EGTA concentration from 0.5 to 5 mM in PC terminals (74 ± 23 fF at terminals on PC and 95 ± 38 fF on DCN neuron, respectively) (Fig. 14), suggesting that transmitter release is tightly coupled to the $Ca^{2+}$ influx.

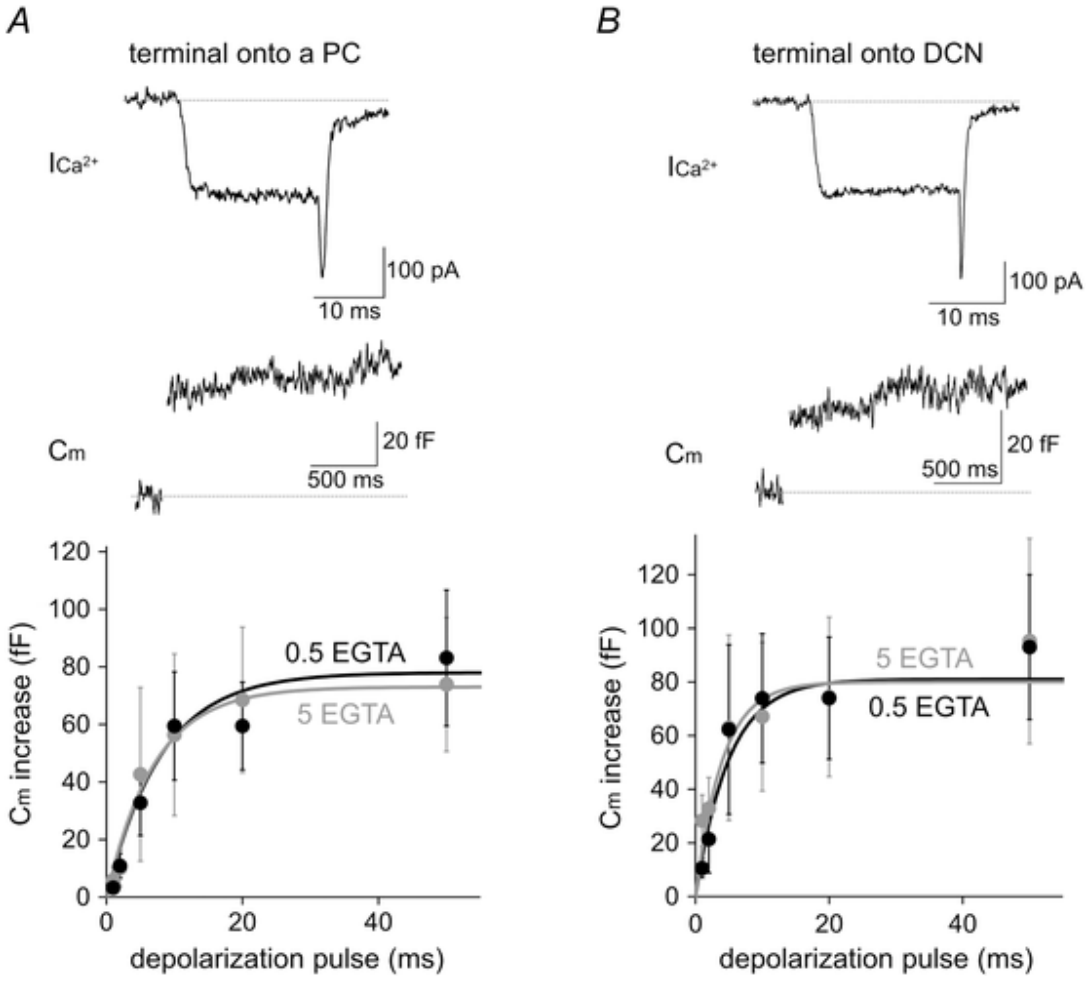


**Figure 14. Cm increases at a PC terminal on a PC or DCN neuron.** Top: representative traces of presynaptic $I_{Ca^{2+}}$ and Cm recorded from a PC terminal on a PC (*A*) or that on a DCN neuron (*B*). Bottom: Cm increases recorded with intracellular 0.5 or 5 mM EGTA were plotted against the depolarization pulse duration [$n = 7$ (0.5 mM EGTA) and $n = 13$ (5 mM EGTA) terminals on a PC; $n = 7$ (0.5 mM EGTA) and $n = 5$ (5 mM EGTA) terminals on a DCN neuron].

Taken all of these results together, we conclude that the $Ca^{2+}$-dependent transmitter release mechanisms and the facilitative property relying on the $Ca^{2+}$-dependent facilitation of $Ca^{2+}$ currents are common in all PC axon terminals. However, because of AP attenuation, PC–DCN synapses exhibit depression rather than facilitation (Kawaguchi and Sakaba, 2015).

# Chapter 4. Discussion

By direct patch clamp recording from inhibitory presynaptic terminals of cultured cerebellar PCs, we have studied a mechanism of PPF at GABAergic synapses between PCs. This technique allowed us to reveal that (1) voltage-gated $Ca^{2+}$ currents were facilitated in a $Ca^{2+}$-dependent manner in PC axon terminals and (2) short-term facilitation of $Ca^{2+}$ currents almost exclusively determines the short-term facilitation of synaptic transmission between PCs. We conclude that PC–PC synapses show short-term facilitation of transmitter release predominantly depending on the $Ca^{2+}$-dependent $Ca^{2+}$ current facilitation. Our data further indicated that the synaptic facilitating property relying on the $Ca^{2+}$ current facilitation was common at PC output synapses, irrespective of the target cells, when identical paired AP commands were applied to the terminal.

## 4.1. Cultured cerebellar cells as a model system

The biophysical properties of the PC – PC synapses in cerebellar cultures here reported are comparable to those from cerebellar slices. The IPSC of PC – PC synapses in slices shows on average an onset delay of 1.62 ms (*culture:* 2.6 ms), a 10-90% rise time of 2.2 ms (*culture:* 2 ms) and the decay could be described by a single exponential function with time constant of 13.3 ms (*culture:* comparable with a half-height width of 15 ms). The slight difference in onset delay may be attributed to the differences in positions between PCs. In slices, PCs are highly organized in a parallel array in the cerebellar cortex, with PC – PC synapses occurring between neighbouring PCs (Watt *et al.*, 2010, Orduz and Llano, 2007, Bornschein *et al.* 2013). However, PCs in our cultures show no fixed pattern, with a mean distance from the axon hillock to the closest synapse of 530 μm, which seems to be approximately two fold of that in slices.

PPF at the PC – PC synapse at high frequencies in our culture preparation (5 ms, 1.50; 10 ms, 1.34) is also comparable to that found in slice experiments (3 ms, 1.79; 10 ms, 1.32, Orduz and Llano, 2007). At lower frequencies, however, the similitude stops (our findings: 20 ms, 1.22, 50 ms, 1.07; Orduz and Llano's finding: 20 ms, no facilitation observed at inter-stimuli interval greater than 20 ms). These differences in

the time courses between the PPR here obtained and those reported in the literature may be due to the differences in EGTA concentration used for the presynaptic cell. Whereas we use a solution with 5 mM EGTA, the one used in the study by Orduz and Llano has 10 mM EGTA. As per our findings (Fig. 10C), EGTA accelerates the decay of PPF and may be the cause of the different PPR recovery time courses.

Further findings of the biophysical properties of PC axon terminals here reported have no counterpart in slices, due to the difficulty in performing the technique (but see Kawaguchi and Sakaba, 2015, for properties of PC axon terminals on DCN neurons in acute slices). As suggested above, development of new recording techniques may provide a framework in which these findings can be replicated and corroborated in slice—or even *in vivo*—preparations.

The PC – PC synapse shifts from depression to facilitation during the developmental stage. It may be interesting to study this transition toward opposite types of plasticity. However, cultured cerebellar cells are not an appropriate model to study this phenomenon using an electrophysiological approach. During the developmental period (until 3-4 weeks after seeding), the majority of the cells are not entirely differentiated, and those that have exhibit very tiny synaptic varicosities. Additionally, the EGFP signal is weak. These three shortcomings prevent the electrophysiological study of the short-term plasticity in this synapse during the early periods of development.

Taken it all together, our results show that cerebellar culture provides an appropriate model for studying the biophysical properties of cells and synapses that can help circumvent some of the problems encountered in slice preparation, such as accessibility of synaptic terminals. It is important to bear in mind, though, that we cannot exclude the possibility that during the culturing process, molecular mechanisms inside the cell may be affected in a significant manner. Thus, support from results performed *in vivo* or in slices is advised for a proper interpretation of the results.

## 4.2. $Ca^{2+}$ current facilitation

In the present study, we demonstrated that $Ca^{2+}$ currents in PC axon terminals are facilitated by ~10% in a $Ca^{2+}$-dependent manner upon high-frequency paired APs.

Previous studies on PPF at PC–PC synapses in slice preparation could not detect facilitated increase in $[Ca^{2+}]_i$ by fluorescence imaging (Orduz and Llano, 2007; Bornschein *et al.* 2013). Considering the tiny fluorescence change by single AP-triggered $Ca^{2+}$ influx as a result of the strong $Ca^{2+}$ buffering (Fig. 12), it appears to be hard to detect a small facilitation of $Ca^{2+}$ influx of ~10% by $Ca^{2+}$imaging. Similar $Ca^{2+}$-dependent facilitation of $Ca^{2+}$ currents has been reported at the glutamatergic presynaptic terminals in the calyx of Held (Forsythe *et al.*, 1998; Borst and Sakmann, 1998; Cuttle *et al.*, 1998), which partly contributes to short-term facilitation of synaptic transmission when the basal release probability is lowered (Felmy *et al.* 2003; Müller *et al.* 2008; Hori and Takahashi, 2009).

CNS neurons have several types of voltage-gated $Ca^{2+}$ channels, such as N, L, P/Q and R-types. Among these, mature PCs express P/Q type $Ca^{2+}$ channels abundantly. Its genetic ablation results in severe ataxia (Jun *et al.* 1999) and reduced synaptic facilitation at the calyx of Held synapse (Inchauspe *et al.* 2004). The detailed mechanism of $Ca^{2+}$-dependent $Ca^{2+}$ current facilitation has been studied using a heterologous expression system (Lee *et al.* 2003; DeMaria *et al.* 2001; Catterall and Few, 2008; Ben-Johny and Yue, 2014). Similar to other types of $Ca^{2+}$channels, the P/Q type has a CaM binding site. The $Ca^{2+}$ binding to C-lobe of CaM is reported to rapidly (<1 ms) facilitate the $Ca^{2+}$ currents by increasing the channel open probability. On the other hand, CaM bound with $Ca^{2+}$ at N-lobe has been shown to inactivate the P/Q type $Ca^{2+}$ channels relatively slowly (tens of milliseconds). In addition, neuronal $Ca^{2+}$ sensor protein was also suggested to mediate the $Ca^{2+}$-dependent facilitation of $Ca^{2+}$ currents in a similar manner to CaM but with stronger $Ca^{2+}$ affinity (Tsujimoto *et al.* 2002). If the $Ca^{2+}$ current is facilitated by a mechanism coupled loosely with the $Ca^{2+}$ influx, an increase of exogenous buffering by EGTA is expected to weaken the $Ca^{2+}$ current facilitation (Naraghi and Neher, 1997, Neher, 1998), because the binding rate of the EGTA is relatively slow ($2.5 \times 10^6$ $M^{-1}s^{-1}$). However, as shown in Figs 7 and 11, a high concentration of EGTA accelerated the recovery moderately and did not change the peak amplitude of $Ca^{2+}$ current facilitation in PC terminals (Alturi and Regehr, 1998). Thus, the $Ca^{2+}$ current facilitation appears to be tightly coupled with local $Ca^{2+}$ influx, which is consistent with the idea that $Ca^{2+}$-binding to CaM associated with the P/Q-type $Ca^{2+}$ channels at rest contributes to $Ca^{2+}$ current facilitation (Erickson *et al.* 2001; Ben-Johny and Yue, 2014). Consistently, BAPTA, a

fast $Ca^{2+}$ chelator (binding rate 4 x $10^8$ $M^{-1}s^{-1}$), blocks $I_{Ca^{2+}}$ facilitation completely.

Interestingly, the $Ca^{2+}$ current facilitation by $Ca^{2+}$/CaM is specific to P/Q-type $Ca^{2+}$ channels, and other types of $Ca^{2+}$ channels are rather inactivated by $Ca^{2+}$/CaM association (Catterall and Few, 2008; Ben-Johny and Yue, 2014). The types of $Ca^{2+}$ channels contributing to transmitter release in presynaptic terminals developmentally change at some synapses, including PC output synapses, excitatory synapses in the calyx of Held and thalamic inhibitory synapses (Iwasaki *et al.* 2000; Miki *et al.* 2013). Thus, short-term plasticity by $Ca^{2+}$ channel modulation might also developmentally change. Indeed, in contrast to PPF at synapses between PCs in slices prepared from postnatal day 7–19 mice (Orduz and Llano, 2007; Bornschein *et al.* 2013), PPD was observed in younger mice (postnatal day 4–6 mice) (Watt *et al.* 2009). A developmental switch of $Ca^{2+}$ channels in the PC terminal from mixture of N-, R- and P/Q-type to P/Q-type-specific (Iwasaki *et al.* 2000) might be responsible for the age-dependent differences in short-term plasticity.

It is important to highlight that the results here obtained are not necessarily exclusive to PC terminals. The majority of neurons in the CNS express P/Q-type VDCCs, which would suggest that the mechanisms here studied may also be present at other synapses. However, different synapses have different interplays of mechanisms mediating both facilitation and depression, as has been observed both here in PC – DCN synapse and in other synapses (see Hori and Takahashi, 2009, for facilitation at the calyx of Held, a usually depressing synapse).

PCs, in particular, express large quantities of endogenous $Ca^{2+}$ buffers compared with other neurons. This large buffering capacity may cause mechanisms such as residual calcium and saturation of endogenous buffers not to take place at PCs, leaving the possibility that the main mechanism for facilitation is limited to $Ca^{2+}$ current facilitation.

## 4.3. Mechanisms of PPF

The averaged PSC amplitude (409 pA) at a PC pair with approximately six synaptic contacts and the miniature PSC amplitude (52 pA) imply that one or two synaptic vesicles are exocytosed at each presynaptic terminal. This estimation is in accordance

with the number of exocytosed vesicles (~2) based on the PSC amplitude (116 pA) upon an AP command at single terminal. Thus, the release probability per synapse is almost 1 in PC terminals. On the other hand, the Cm measurement suggests that ~1000 vesicles are readily releasable in a single terminal within 10 ms if a strong $Ca^{2+}$ increase takes place (Fig. 14). Thus, the release probability per each RRP vesicle is estimated to be very low (~0.2%). It should be noted that the number of synaptic vesicles exocytosed upon a square depolarization pulse might be larger than the releasable vesicle pool upon high frequency APs, because of massive $Ca^{2+}$ influx. In addition, if the vesicle replenishment is very fast (i.e. several milliseconds) (Valera *et al.* 2012; Brachtendorf *et al.* 2015), the capacitance measurement might overestimate the RRP size by 2- to 3-fold. In any cases, a PC axon terminal has a large amount of RRP vesicles and the release probability of each release-ready vesicle upon an AP is low. The large RRP and low release probability are typical properties of facilitating synapses (Dittman *et al.* 2000) and the increase of release probability leads to PPF.

Paired recordings from a PC axon terminal and a postsynaptic PC soma demonstrated that PPF is almost exclusively mediated by the $Ca^{2+}$-dependent facilitation of $Ca^{2+}$ current into a presynaptic terminal (Figs 4 and 5). Using the expression of mutant $Ca^{2+}$ channels in cultured superior cervical ganglion neurons, a tight correlation between $Ca^{2+}$ current modulation and short-term plasticity was demonstrated (Mochida *et al.* 2008). When the release probability is decreased to suppress depletion of the releasable synaptic vesicle pool, the calyx of Held synapses also show short-term facilitation, ~50% of which relies on the $Ca^{2+}$-dependent $Ca^{2+}$ current facilitation (Felmy *et al.* 2003; Müller *et al.* 2008; Hori and Takahashi, 2009). Thus, $Ca^{2+}$-dependent $Ca^{2+}$ current facilitation may contribute to synaptic facilitation at many synapses. However, our data do not necessarily exclude other mechanisms suggested in PPF at other synapses. The residual $Ca^{2+}$ hypothesis is the most straightforward, commonly accepted one arising from studies on short-term facilitation at the neuromuscular junction (Katz and Miledi,1968). It was postulated that the summation of residual $Ca^{2+}$ remaining in the cytoplasm after the first AP and the local $Ca^{2+}$ during the following AP contributes to the facilitated transmitter release as a result of the 4th power dependence of transmitter release on $[Ca^{2+}]_i$. However, in most cases, the residual $[Ca^{2+}]_i$ increase is estimated to be too small compared to the local $[Ca^{2+}]_i$ to account for facilitation. This is particularly the

case for PC axon terminals (Fig. 12) (Orduz and Llano, 2007), presumably as a result of very high expression of high affinity $Ca^{2+}$ buffer calbindin. We estimated that the residual $[Ca^{2+}]_i$ increase accounts for only 1–2% facilitation at PC–PC synapses.

Saturation of mobile $Ca^{2+}$ buffer proteins in presynaptic terminals has also been considered as a candidate mechanism for short-term facilitation. If $Ca^{2+}$ entering into the terminal upon the first AP remains bound to the large part of $Ca^{2+}$ buffer molecules, free $[Ca^{2+}]_i$ is expected to become higher upon the following APs, leading to larger transmitter release (Rozov *et al.*, 2001). Indeed, calbindin was shown to contribute to the PPF at inhibitory synapses in the cerebral cortex and excitatory mossy fibre–CA3 synapses in the hippocampus (Blatow *et al.* 2003). On the other hand, despite extensive expression of calbindin in cerebellar PCs throughout the cell, it was recently demonstrated that PPF at PC–PC synapses was not affected by the genetic ablation of either calbindin or parvalbumin, another $Ca^{2+}$ buffer protein (Bornschein *et al.*2013). The lack of effect by calbindin ablation on PPF might be a result of the limited amount of $Ca^{2+}$ influx into the presynaptic terminal upon a single AP (half-width of ~0.4 ms) (Fig. 9), which might be far from saturating the abundant calbindin. Also, the buffer saturation model requires loose coupling between $Ca^{2+}$ channels and vesicles (Neher, 1998; Rozov *et al.*, 2001; Vyleta and Jonas, 2014), which is not the case at this (Fig. 14) and other inhibitory synapses (Bucurenciu *et al.* 2008), given that transmitter release is EGTA-insensitive.

Another hypothesis is that $Ca^{2+}$ causes facilitation acting at presynaptic release sensors (Atluri and Regehr, 1998; Bertram *et al.*, 1996; Regehr, 2012). If there is a $Ca^{2+}$-binding site for release with high $Ca^{2+}$ affinity and slow kinetics, the site is expected to be occupied with $Ca^{2+}$ during the small increase of residual $Ca^{2+}$, resulting in facilitated release upon the following stimulation. However, the identity of the molecule playing this role remains obscure. Using a kinetic simulation based on the five-site $Ca^{2+}$ sensor model (Schneggenburger and Neher, 2000), the slow and high-affinity $Ca^{2+}$ sensor for vesicular release was suggested to underlie the PPF observed at PC–PC synapses (Bornschein *et al.* 2013). By contrast, we now show that the PPF of PSCs is suppressed when the amplitude of $Ca^{2+}$ current upon the second AP is identical to that upon the first (Fig. 11), indicating that the first $Ca^{2+}$ influx exerts little positive effect on the release machinery remaining at the time of next AP arrival. Alternatively, we demonstrate that the $Ca^{2+}$-dependent $Ca^{2+}$ current facilitation plays

a role as a '$Ca^{2+}$ sensor' for the PPF at PC–PC synapses.

Activity-dependent recruitment of an extra pool or reluctant vesicles to the RRP is also a possible mechanism for PPF (Valera *et al.* 2012; Brachtendorf *et al.* 2015). However, our Cm measurement data showing the uniform releasable vesicle pool in PC terminals imply that RRP size change may not be implicated in the PPF at PC–PC synapses.

## 4.4. Target-dependent plasticity and physiological implication

We demonstrated that the $Ca^{2+}$-dependent facilitation of $Ca^{2+}$ currents and the resultant synaptic short-term facilitation are a common property of PC terminals irrespective of their target neurons (i.e. another PC or DCN cells) when the amplitudes of APs are identical (using AP commands). In accordance with a previous study on PC terminals on a DCN neuron (Kawaguchi and Sakaba, 2015), PC terminals on another PC also exhibited the large readily releasable synaptic vesicle pool (~1000 vesicles) and the low release probability (<1%) upon an AP arrival, which are typical properties of facilitating synapses (Dittman *et al.* 2000). However, PC–PC synapses exhibit short-term facilitation (Orduz and Llano, 2007; Bornschein *et al.* 2013), whereas PC–DCN synapses undergo short-term depression *in situ* (Telgkamp and Raman, 2002). These apparently opposite directions of plasticity dependent on the target neurons can simply be explained by the difference in AP conduction fidelity. Direct recordings from an axon and/or a terminal previously demonstrated that AP amplitudes attenuated around axon terminals on DCN neurons located far from the PC soma in both culture and slice preparation (Kawaguchi and Sakaba, 2015). On the other hand, previous studies have shown that axonal AP conduction from the soma to the proximal region of axon is reliable up to 200 Hz (Khaliq and Raman, 2005; Monsivais *et al.* 2005). Consistently, our preliminary data suggest that an AP train at 100 Hz faithfully propagates from the soma to the proximal terminal on a PC with little attenuation of amplitude (Shin-ya Kawaguchi, unpublished observation). Consequently, the PC–PC synapses exhibit short-term facilitation through the facilitated $Ca^{2+}$current. On the other hand, taking the 4th power dependence of synaptic transmission on the $Ca^{2+}$ current (Fig. 8) into consideration, a small decrease of $Ca^{2+}$ influx caused by a slight AP amplitude change has a large impact on synaptic

efficacy, converting the intrinsically facilitating synapses to depressing synapses at PC–DCN synapses.

Target-dependent short-term synaptic plasticity has been reported at various synapses, such as those in neocortex, cerebellum and hippocampus (Markram *et al.* 1998; Rozov *et al.* 2001; Koester and Johnston, 2005; Pelkey *et al.* 2006; Beierlein *et al.* 2007; Bao *et al.* 2010). For example, excitatory synapses from a cortical pyramidal neuron on basket cells exhibit short-term depression, whereas those on Martinotti cells show facilitation (Markram *et al.* 1998). It is generally assumed that synapses usually contain both the mechanisms for facilitation and those for depression, and transmitter release probability is considered to determine which of the two mechanisms prevails. Fluorescence imaging techniques have shown that the facilitating presynaptic varicosities tend to show a small $Ca^{2+}$ increase and low synaptic release probability, whereas the depressing ones show larger $Ca^{2+}$ transients and higher release probability (Koester and Johnston, 2005). Considering the large impact of AP amplitude on the presynaptic $Ca^{2+}$ influx and the resultant synaptic transmission, we suggest that slight differences of membrane excitability in presynaptic terminals may also play a role in the target-dependent plasticity. To test this idea at various synapses in the future, direct recording from the terminals and/or development of voltage-sensitive dyes are essential (Hoppa *et al.* 2014; Vyleta and Jonas, 2014).

## 4.5. Physiological importance of PC – PC connection

Given that PCs are among the earliest neurons to migrate into the cerebellar cortex (Sotelo, 2004), they may play an important role in the development of the synaptic circuitry of the young cerebellar cortex. Axon collaterals of PCs are particularly abundant in the early stages of development, and are pruned to a mature distribution by the third week of postnatal development (Gianola *et al.*, 2003). This may suggest that PC – PC synapses may be particularly important during the first postnatal week, at a time when basket and stellate cell synaptic inputs onto PC are not yet fully established (Watt *et al.*, 2009). During late development, at around two to three weeks, only a limited number of PC axon collaterals remain (Orduz and Llano, 2007). The remaining PC – PC synapses exhibit short-term facilitation upon high frequencies. At

this point, PF – PC synapses, as well as the synapses from the inhibitory interneuron are in place (Dusart and Flamant, 2012).

What may be then the function of the PC – PC synapse during this late developmental stage? It is known that groups of PCs aligned along the direction of the parallel fibers fire simple spikes synchronously upon peripheral stimulation (Ebner and Bloedel, 1981). The inhibitory prevalent nature of PC–PC synapses could contribute to sharpen the boundaries of such PC domains (Orduz and Llano, 2007). The PC – PC connection may work as a spatial delimiter.

Another possibility is related to the synchronicity of PC firing. Recently, evidence that subsets of PCs synchronize their firing during behaviors that require the cerebellum has been reported, and it has been proposed that that synchronous inhibitory input from PCs can set the timing and rate of action potentials produced by DCN cells, thereby relaying information out of the cerebellum (Person and Raman, 2012). If this were the case, then modifying the spatiotemporal patterns of PC activity would allow different subsets of inhibitory neurons to control cerebellar output at different times. An inhibitory high-pass filter, caused by the PPF of the PC – PC connection, may help modulating the subsets of PCs to shape the pattern of activity at PC level, and thus the activity of the DCN, by modifying in a non-discreet manner the firing patterns of some of the PCs of the network.

A third possibility is to make travelling waves of activity especially during development. It has been reported that in several CNS regions, spontaneous traveling waves of activity early in development are critical in establishing the accurate synaptic connectivity of mature circuits (Feller, 1999, Katz and Shatz, 1996). The PC – PC connection has been shown to provide a robust substrate for propagating waves of activity in the early developing cerebellum (Watt *et al.*, 2009).

A proper understanding of the role of the short-term facilitation and the PC – PC synapse in the development of the cerebellar circuitry requires further research at a larger scale (cerebellar network). One approach would be by the genetic ablation of P/Q-type VDCC (Giogovaz-Tropper *et al.*, 2011) or replacement by overexpression of N-type VDCC (Cao and Tsien, 2010). However, this leaves the possibility that depression would replace facilitation at this synapse, as is the case in earlier developmental stages. Given that knockout of CaM, a strong candidate for the mechanisms

underlying facilitation of P/Q-type VDCC, leads to cell death (Panina *et al.*, 2012), elimination of the PPF property in the young cerebellum whilst preserving P/Q-type VDCC may be hard to achieve. Perhaps a first approach to this problem can be achieved by software modeling of the cerebellar circuitry (Kobayashi *et al.*, 1998, Kawato 2009). Present models of the cerebellum circuit, however, exclude the PC – PC connection. It would be then interesting to model a young cerebellar cortex in which PC – PC synapses are still present.

# Chapter 5. References


1. Abbott LF & Regehr WG (2004). Synaptic computation. *Nature* **431**, 796–803.
2. Atluri PP & Regehr WG (1996). Determinants of the time course of facilitation at the granule cell to Purkinje cell synapse. *J Neurosci* **16**, 5661–5671.
3. Atluri PP & Regehr WG (1998). Delayed release of neurotransmitter from cerebellar granule cells. *J Neurosci* **18**, 8214–8227.
4. Augustine GJ & Charlton MP (1986). Calcium dependence of presynaptic calcium current and post-synaptic response at the squid giant synapse. *J Physiol.* **381**, 619–640.
5. Bain AI & Quastel DM (1992). Multiplicative and additive $Ca^{2+}$-dependent components of facilitation at mouse endplates. *J Physiol* **455**, 383–405.
6. Bao J, Reim K & Sakaba T (2010). Target-dependent feedforward inhibition mediated by short-term synaptic plasticity in the cerebellum. *J Neurosci* **30**, 8171–8179.
7. Bastianelli E (2003). Distribution of calcium-binding proteins in the cerebellum. *Cerebellum* **2**, 242–262.
8. Beierlein M, Fioravante D & Regehr WG (2007). Differential expression of posttetanic potentiation and retrograde signaling mediate target-dependent short-term synaptic plasticity. *Neuron* **54**, 949–959.
9. Ben-Johny M & Yue DT (2014). Calmodulin regulation (calmodulation) of voltage-gated calcium channels. *J Gen Physiol* **143**,679–692.
10. Bertram R, Sherman A & Stanley EF (1996). Single-domain/bound calcium hypothesis of transmitter release and facilitation. *J Neurophysiol* **75**, 1919–1931.
11. Betz WJ (1970). Depression of transmitter release at the neuromuscular junction of the frog. *J Physiol* **206**, 629–644.
12. Blatow M, Caputi A, Burnashev N, Monyer H & Rozov A (2003). $Ca^{2+}$ buffer saturation underlies paired pulse facilitation in calbindin-D28k-containing terminals. *Neuron* **38**, 79–88.
13. Bornschein G, Arendt O, Hallermann S, Brachtendorf S, Eilers J & Schmidt H (2013). Paired-pulse facilitation at recurrent Purkinje neuron synapses is independent of calbindin and parvalbumin during high-frequency activation. *J Physiol* **591**, 3355–3370.
14. Borst JG & Sakmann B (1998). Facilitation of presynaptic calcium currents in the rat brainstem. *J Physiol* **513**, 149–155.

15. Brachtendorf S, Eilers J & Schmidt H (2015). A use-dependent increase in release sites drives facilitation at calretinin-deficient cerebellar parallel-fiber synapses. *Front Cell Neurosci.* **9**, 27.

16. Branchaw JL, Banks MI & Jackson MB (1997). $Ca^{2+}$- and voltage-dependent inactivation of $Ca^{2+}$ channels in nerve terminals of the neurohypophysis. *J Neurosci* **17**, 5772–5781.

17. Branco T & Staras K (2009). The probability of neurotransmitter release: variability and feedback control at single synapses. *Nature Rev Neurosci* **10**, 373-383.

18. Bucurenciu I, Kulik A, Schwaller B, Frotscher M & Jonas P (2008). Nanodomain coupling between $Ca^{2+}$ channels and $Ca^{2+}$ sensors promotes fast and efficient transmitter release at a cortical GABAergic synapse. *Neuron* **57**, 536–545.

19. Buonomano DV (2000). Decoding temporal information: a model based on short-term synaptic plasticity. *J Neurosci* **20**, 1129–1141.

20. Caillard O, Moreno H, Schwaller B, Llano I, Celio MR & Marty A (2000). Role of the calcium-binding protein parvalbumin in short-term synaptic plasticity. *Proc Natl Acad Sci* **97**, 13372–13377.

21. Cao YQ & Tsien RW. Different relationship of N- and P/Q-type $Ca^{2+}$ channels to channel-interacting slots in controlling neurotransmission at cultured hippocampal synapses. *J Neurosci* **30**, 4536-46.

22. Catterall WA & Few AP (2008). Calcium channel regulation and presynaptic plasticity. *Neuron* **59**, 882–901.

23. Cull-Candy S, Brickley S & Farrant M (2001). NMDA receptor subunits: diversity, development and disease. *Curr Opin Neurobiol* **3**, 327-335.

24. Currie KP (2010). G protein modulation of CaV2 voltage-gated calcium channels. *Channels (Austin)* **4**, 497-509.

25. Cuttle MF, Tsujimoto T, Forsythe ID & Takahashi T (1998). Facilitation of the presynaptic calcium current at an auditory synapse in rat brainstem. *J Physiol* **512**, 723–729.

26. Delgado R, Maureira C, Oliva C, Kidokoro Y & Labarca P (2000). Size of vesicle pools, rates of mobilization, and recycling at neuromuscular synapses of a Drosophila mutant, shibire. *Neuron* **28**, 941–953.

27. DeMaria CD, Soong TW, Alseikhan BA, Alvania RS & Yue DT (2001). Calmodulin bifurcates the local $Ca^{2+}$ signal that modulates P/Q-type $Ca^{2+}$ channels. *Nature* **411**, 484–489.

28. Dingledine R, Borges K, Bowie D & Traynelis SF (1999). The Glutamate Receptor Ion Channels. *Pharmacol Rev* **51**, 7-62.

29. Dittman JS, Kreitzer AC & Regehr WG (2000). Interplay between facilitation, depression, and residual calcium at three presynaptic terminals. *J Neurosci* **20**, 1374–1385.

30. Dusart I & Flamant F (2012) Profound morphological and functional changes of rodent Purkinje cells between the first and the second postnatal weeks: a metamorphosis?. *Front. Neuroanat* **6**, 11.

31. Ebner TJ & Bloedel JR (1981). The action of climbing fibers on Purkinje cell responsiveness to mossy fiber inputs. *Advances in Physiological Science*, **198**--1. G. Adam, I. Meszaros & E. I. Banyai (eds.).

32. Erickson MG, Alseikhan BA, Peterson BZ & Yue DT (2001). Preassociation of calmodulin with voltage-gated Ca(2+) channels revealed by FRET in single living cells. *Neuron* **31**, 973–985.

33. Fatt P & Katz B (1952), Spontaneous subthreshold activity at motor nerve endings. *J Physiol* **117**, sp004735.

34. Feller MB (1999). Spontaneous correlated activity in developing neural circuits. *Neuron* **22**, 653-6.

35. Felmy F, Neher E & Schneggenburger R (2003). Probing the intracellular calcium sensitivity of transmitter release during synaptic facilitation. *Neuron* **37**, 801–811.

36. Fioravante D & Regehr WG (2011). Short-term forms of presynaptic plasticity. *CurrOpinNeurobiol* **21**, 269–274.

37. Fisher S, Fischer T & Carew T (1997). Multiple overlapping processes underlying short-term synaptic enhancement. *Trends Neurosci* **20**, 170-7.

38. Forsythe ID, Tsujimoto T, Barnes-Davies M, Cuttle MF & Takahashi T (1998). Inactivation of presynaptic calcium current contributes to synaptic depression at a fast central synapse. *Neuron* **20**, 797–807.

39. Fortune ES & Rose GJ (2001). Short-term synaptic plasticity as a temporal filter. *Trends Neurosci* **24**, 381–385.

40. Geiger JR & Jonas P (2000). Dynamic control of presynaptic $Ca^{2+}$ inflow by fast-inactivating K(+) channels in hippocampal mossy fiber boutons. *Neuron* **28**, 927–939.

41. Gianola S, Savio T, Schwab ME & Rossi F (2003) Cell-autonomous mechanisms and myelin-associated factors contribute to the development of Purkinje axon intracortical plexus in the rat cerebellum. *J Neurosci* **23**, 4613–4624.

42. Giugovaz-Tropper B, González-Inchauspe C, Di Guimi MN, Urbano FJ, Forsythe ID & Uchitel OD (2011). P/Q-type calcium channel ablation in a mice glycinergic synapse mediated by multiple types of Ca(2+) channels alters transmitter release and short term plasticity. *Neurosci* **192**, 219–230.

43. Hevers W & Lüddens H (1998). The diversity of GABAA receptors. Pharmacological and electrophysiological properties of GABAA channel subtypes. *Mol Neurobiol* **18,** 35-86.

44. Hoppa MB, Gouzer G, Armbruster M & Ryan TA (2014). Control and plasticity of the presynaptic action potential waveform at small CNS nerve terminals. *Neuron* **84**, 778–789.

45. Hori T & Takahashi T (2009). Mechanisms underlying short-term modulation of transmitter release by presynaptic depolarization. *J Physiol* **587**, 2987–3000.

46. Inchauspe CG, Martini FJ, Forsythe ID & Uchitel OD (2004). Functional compensation of P/Q by N-type channels blocks short-term plasticity at the calyx of held presynaptic terminal. *J Neurosci* **24**, 10379–10383.

47. Ishikawa T, Kaneko M, Shin HS & Takahashi T (2005). Presynaptic N-type and P/Q-type $Ca^{2+}$ channels mediating synaptic transmission at the calyx of Held of mice. *J Physiol* **568**, 199–209.

48. Ivry R (1997). Cerebellar timing systems. *Int Rev Neurobiol* **41**, 555-73.

49. Iwasaki S, Momiyama A, Uchitel OD & Takahashi T (2000). Developmental changes in calcium channel types mediating central synaptic transmission. *J Neurosci* **20**, 59–65.

50. Izhikevich EM, Desai NS, Walcott EC, Hoppensteadt FC (2003). Bursts as a unit of neural information: selective communication via resonance. *Trends Neurosci* **26**, 161–167.

51. Jackson MB, Konnerth A & Augustine GJ (1991). Action potential broadening and frequency-dependent facilitation of calcium signals in pituitary nerve terminals. *Proc Natl Acad Sci USA.* **88**, 380–384.

52. Jahn R, Lang T & Sudhof TC. 2003. Membrane fusion. Cell **112**, 519–533.

53. Jun K, Piedras-Rentería ES, Smith SM, Wheeler DB, Lee SB, Lee TG, Chin H, Adams ME, Scheller RH, Tsien RW & Shin HS (1999).Ablation of P/Q-type Ca(2+) channel currents, altered synaptic transmission, and progressive ataxia in mice lacking the alpha(1A)-subunit. *Proc Natl Acad Sci USA* **96**, 15245–15250.

54. Kaeser PS & Regehr WG (2014). Molecular Mechanisms for Synchronous, Asynchronous, and Spontaneous Neurotransmitter Release. *Annu Rev Physiol* **76**, 333-363.

55. Kamiya H & Zucker RS (1994). Residual $Ca^{2+}$ and short-term synaptic plasticity. *Nature* **371**, 603–606.

56. Kaneko M, Yamaguchi K, Eiraku M, Sato M, Takata N, Kiyohara Y, Mishina M, Hirase H, Hashikawa T & Kengaku M (2011).Remodelling of monoplaner Purkinje cell dendrites during cerebellar circuit formation. *Plos ONE* e20108.

57. Katz B & Miledi R (1968). The role of calcium in neuromuscular facilitation. *J Physiol* **195**, 481–492.

58. Katz LC & Shatz CJ (1996). Synaptic activity and the construction of cortical circuits. *Science* **274**, 1133-8.

59. Kawaguchi S & Hirano T (2007). Sustained structural change of $GABA_A$ receptor-associated protein underlies long-term potentiation at inhibitory synapses on a cerebellar Purkinje neuron. *J Neurosci* **27**, 6788–6799.

60. Kawaguchi S & Sakaba T (2015). Control of inhibitory synaptic outputs by low excitability of axon terminals revealed by direct recording. *Neuron* **85**,1273-1288.

61. Kawato M (2009) Cerebellum: Models. *Encyclopedia of Neuroscience*, **2**, 757-767. Oxford: Academic Press. Squire LR (ed.).

62. Khaliq ZM6 Raman IM (2005). Axonal propagation of simple and complex spikes in cerebellar Purkinje neurons. *J Neurosci* **25**,454–463.

63. Kits KS & Mansvelder HD (2000). Regulation of exocytosis in neuroendocrine cells: spatial organization of channels and vesicles, stimulus-secretion coupling, calcium buffers and modulation. *Brain Res Rev* **33**, 78-94.

64. Kobayashi Y, Kawano K, Takemura A, Inoue Y, Kitama T, Gomi H, Kawato M (1998) Temporal firing patterns of Purkinje cells in the cerebellar ventral paraflocculus during ocular following responses in monkeys. II. Complex spikes. J Neurophysiol **80**, 832–848.

65. Koester HJ & Johnston D (2005). Target cell-dependent normalization of transmitter release at neocortical synapses. *Science* **308**,863–866.

66. Konnerth A, Liano I & Armstrong CM (1990). Synaptic currents in cerebellar Purkinje cells. *Proc Natl Acad Sci USA* **87**, 2662–2665.

67. Lee A, Zhou H, Scheuer T & Catterall WA (2003). Molecular determinants of Ca(2+)/calmodulin-dependent regulation of Ca(v)2.1 channels. *Proc Natl Acad Sci USA* **100**, 16059–16064.

68. Liley AW & North KA (1953). An electrical investigation of effects of repetitive stimulation on mammalian neuromuscular junction. *J Neurophysiol* **16**, 509–527.

69. Lin JW, Sugimori M, Llinás RR, McGuinness TL & Greengard P (1990). Effects of synapsin I and calcium/calmodulin-dependent protein kinase II on spontaneous neurotransmitter release in the squid giant synapse. *Proc Natl Acad Sci* **87**, 8257-8261.

70. Liu T, D. Xu, Ashe J & Bushara K (2008). Specificity of Inferior Olive Response to Stimulus Timing. *J Neurophysiol* **100**, 1557-1561.

71. Llinás R, Sugimori M, Lin JW, Cherksey B (1989). Blocking and isolation of a calcium channel from neurons in mammals and cephalopods utilizing a toxin fraction (FTX) from funnel-web spider poison. Proc Natl Acad Sci U S A. **86**, 1689-93.

72. Macdonald RL & Olsen RW (1994). GABAA Receptor Channels. *Annu Rev Neurosci* **17**, 569-602.

73. Markram H, Wang Y & Tsodyks M. (1998). Differential signaling via the same axon of neocortical pyramidal neurons. *Proc Natl Acad Sci USA* **95**, 5323–5328.

74. Matveev V, Zucker RS & Sherman A (2004). Facilitation through buffer saturation: constraints on endogenous buffering properties. *Biophys J* **86**, 2691–2709.

75. Meldrum BS (2000). Glutamate as a neurotransmitter in the brain: review of physiology and pathology. *J Nutr* **130**, 1007S-15S.

76. Miki T, Hirai H & Takahashi T (2013). Activity-dependent neurotrophin signaling underlies developmental switch of $Ca^{2+}$ channel subtypes mediating neurotransmitter release. *J Neurosci* **33**, 18755–18763.

77. Mochida S, Few AP, Scheuer T & Catterall WA (2008). Regulation of presynaptic Ca(V)2.1 channels by $Ca^{2+}$ sensor proteins mediates short-term synaptic plasticity. *Neuron* **57**, 210–216.

78. Monsivais P, Clark BA, Roth A & Häusser M (2005). Determinants of action potential propagation in cerebellar Purkinje cell axons. *J Neurosci* **25**, 464–472.

79. Muller M, Felmy F, Schwaller B & Schneggenburger R (2007). Parvalbumin is a mobile presynaptic $Ca^{2+}$ buffer in the calyx of Held that accelerates the decay of $Ca^{2+}$ and short-term facilitation. *J Neurosci* **27**, 2261–2271.

80. Müller M, Felmy F & Schneggenburger R (2008). A limited contribution of $Ca^{2+}$ current facilitation to paired-pulse facilitation of transmitter release at the rat calyx of Held. *J Physiol* **586**, 5503–5520.

81. Naraghi M & Neher E (1997). Linearized buffered Ca2+ diffusion in microdomains and its implications for calculation of [Ca2+] at the mouth of a calcium channel. *J Neurosci* **17**, 6961-73.

82. Neher E & Augustine GJ (1992). Calcium Gradients and Buffers in Bovine Chromaffin Cells. *J Physiol.* **450,** 273-301.

83. Neher E & Sakaba T (2001). Estimating transmitter release rates from postsynaptic current fluctuations. *J Neurosci* **21**, 9638–9654.

84. Neher E & Marty A (1982). Discrete changes of cell membrane capacitance observed under conditions of enhanced secretion in bovine adrenal chromaffin cells. *Proc Natl Acad Sci USA* **79**, 6712–6716.

85. Neher E (1998). Vesicle pools and $Ca^{2+}$ microdomains: new tools for understanding their roles in neurotransmitter release. *Neuron***20**, 389–399.

86. Nimmrich V & Gross G (2012). P/Q-type calcium channel modulators. *Br J Pharmacol* **167**, 741-59.

87. O'Donovan MJ & Rinzel J (1997). Synaptic depression, a dynamic regulator of synaptic communication with varied functional roles. *Trends Neurosci* **20**, 431–433.

88. Ohtsuki G, Piochon C & Hansel C (2009). Climbing fiber signaling and cerebellar gain control. *Front Cell Neurosci* **3**, 4.

89. Orduz D & Llano I (2007). Recurrent axon collaterals underlie facilitating synapses between cerebellar Purkinje cells. *Proc Natl Acad Sci USA* **104**, 17831–17876.

90. Pedroarena CM & Schwarz C (2003). Efficacy and short-term plasticity at GABAergic synapses between Purkinje and deep cerebellar nuclei neurons. *J Neurophys* **89**, 704–716.

91. Pelkey KA, Topolnik L, Lacaille JC & McBain CJ (2006). Compartmentalized $Ca^{2+}$ channel regulation at divergent mossy-fiber release sites underlies target cell-dependent plasticity. *Neuron* **52**, 497–510.

92. Perkel DJ, Hestrin S, Sah P & Nicoll RA (1990). Excitatory synaptic currents in Purkinje cells. *Proc Biol Sci.* **241**, 116–121.

93. Person AL & Raman IM (2011). Purkinje neuron synchrony elicits time-locked spiking in the cerebellar nuclei. *Nature* **481**, 502-5.

94. Regehr WG (2012). Short-term synaptic plasticity. *Cold Spring Harb Perspect Biol* **4**, a005702.

95. Richards DA, Guatimosim C, Rizzoli SO & Betz WJ (2003). Synaptic vesicle pools at the frog neuromuscular junction. *Neuron* **39**, 529–541.

96. Rizolli SO & Betz WJ (2005). Synaptic vesicle pools. *Nat Rev Neurosci* **6**, 57-69.

97. Rozov A, Burnashev N, Sakmann B & Neher E (2001). Transmitter release modulation by intracellular $Ca^{2+}$ buffers in facilitating and depressing nerve terminals of pyramidal cells in layer 2/3 of the rat neocortex indicates a target cell-specific difference in presynaptic calcium dynamics. *J Physiol* **531**, 807–826.

98. Sakaba T & Neher E (2001). Quantitative Relationship between Transmitter Release and Calcium Current at the Calyx of Held Synapse. *J Neurosci* **21**,462-476.

99. Scheuss V & Neher E (2001). Estimating synaptic parameters from mean, variance, and covariance in trains of synaptic responses. *Biophys J* **81**, 1970–1989.

100. Schmidt H, Stiefel KM, Racay P, Schwaller B & Eilers J (2003). Mutational analysis of dendritic $Ca^{2+}$ kinetics in rodent Purkinje cells: role of parvalbumin and calbindin D28k. *J Physiol* **551**, 13–32.

101. Schneggenburger R & Neher E (2000). Intracellular calcium dependence of transmitter release rates at a fast central synapse. *Nature* **406**, 889–893.

102. Silver RA (2010). Neuronal arithmetic. *Nature Rev Neurosci* **11**, 474-489.

103. Simpson JI, Wylie DR, de Zeeuw CI. (1996). On climbing fiber signals and their consequence(s). *Behav Brain Sci* **19**, 384–398

104. Sotelo C (2004), Cellular and genetic regulation of the development of the cerebellar system, *Prog Neurobiol* **72**, 295-339.

105. Stanley EF (1984). The action of cholinergic agonists on the squid stellate ganglion giant synapse. *J Neurosci* **4**, 1904–1911.

106. Stopfer M & Carew TJ (1996). Heterosynaptic facilitation of tail sensory neuron synaptic transmission during habituation in tail-induced tail and siphon withdrawal reflexes of aplysia. *J Neurosci* **16**, 4933-4948.

107. Sudhof TC & Rothman JE. 2009. Membrane fusion: Grappling with SNARE and SM proteins. *Science* **323**, 474–477.

108. Südhof TC (2013). A molecular machine for neurotransmitter release: synaptotagmin and beyond. *Nature Medicine* **19**, 1227–1231.

109. Tank DW, Regehr WG & Delaney KR (1995). A quantitative analysis of presynaptic calcium dynamics that contribute to short-term enhancement. *J Neurosci* **15**, 7940–7952.

110. Telgkamp P & Raman IM (2002). Depression of inhibitory synaptic transmission between Purkinje cells and neurons of the cerebellar nuclei. *J Neurosci* **22**, 8447–8457.

111. Thomson AM (2000) Facilitation, augmentation, and potentiation at central synapses. *Trends Neurosci* **23**, 305–312.

112. Tsujimoto T, Jeromin A, Saitoh N, Roder JC & Takahashi T (2002). Neuronal calcium sensor 1 and activity-dependent facilitation of P/Q-type calcium currents at presynaptic nerve terminals. *Science* **295**, 2276–2279.

113. Valera AM, Doussau F, Poulain B, Barbour B & Isope P (2012). Adaptation of granule cell to Purkinje cell synapses to high-frequency transmission. *J Neurosci* **32**, 3267–3280.

114. Varela JA, Sen K, Gibson J, Fost J, Abbott LF, Nelson SB (1997). A quantitative description of short-term plasticity at excitatory synapses in layer 2/3 of rat primary visual cortex. *J Neurosci* **17**, 7926–7940.

115. Varela JA, Song S, Turrigiano GG & Nelson SB (1999). Differential depression at excitatory and inhibitory synapses in visual cortex. *J Neurosci* **19**, 4293–4304.

116. Volman V, Levine H, Ben-Jacob E, Sejnowski TJ (2009). Locally Balanced Dendritic Integration by Short-Term Synaptic Plasticity and Active Dendritic Conductances. *J Neurophysiol* **102**, 3234–3250.

117. Vyleta NP & Jonas P (2014). Loose coupling between $Ca^{2+}$ channels and release sensors at a plastic hippocampal synapse. *Science* **343**, 665–670.

118. Watt AJ, Cuntz H, Mori M, Nusser Z, Sjöström PJ & Häusser M (2009). Traveling waves in developing cerebellar cortex mediated by asymmetrical Purkinje cell connectivity. *Nat Neurosci* **12**, 463–473.

119. Xu D, Liu T, Ashe J & Bushara K (2006). Role of the Olivo-Cerebellar System in Timing. *J Neurosci* **26**, 5990-5995.

120. Xu J & Wu LG. (2005). The decrease in the presynaptic calcium current is a major cause of short-term depression at a calyx-type synapse. *Neuron* **46**, 633–645.

121. Yamada WM & Zucker RS (1992). Time course of transmitter release calculated from simulations of a calcium diffusion model. *Biophys J* **61**, 671–682.

122. Yang H & Xu-Friedman MA (2013). Stochastic properties of neurotransmitter release expand the dynamic range of synapses. *J Neurosci* **33**, 14406-14416.

123. Zucker RS & Fogelson AL. Relationship between transmitter release and presynaptic calcium influx when calcium enters through discrete channels. *Proc Natl Acad Sci U S A* **83**, 3032–3036.

124. Zucker RS & Regehr WG (2002). Short-term synaptic plasticity. *Ann Rev Physiol* **64**, 355–405.